Energy, Mines and Resources Canada
Earth Physics Branch
1 Observatory Crescent
Ottawa Canada
K1A 0Y3

Énergie, Mines et Ressources Canada
Direction de la physique du globe
1 Place de l'Observatoire
Ottawa Canada
K1A 0Y3

Geodynamics Service of Canada

Service de la géodynamique du Canada

THE SEISMIC TRAVELTIME DROP IN THE CHARLEVOIX REGION FROM 1979 to 1980: EVIDENCE FOR ALIGNED, SATURATED CRACKS IN THE CRUST

R. Kirsch, G.G.R. Buchbinder
and A. Lambert

DOSSIER PUBLIC DE LA DIRECTION DE LA PHYSIQUE DU GLOBE 85-36
EARTH PHYSICS BRANCH OPEN FILE NUMBER 85-36

pages : 40
price : $11.63

Abstract

A significant drop in seismic traveltimes of up to 0.5% occurred in the Chalevoix region between 1979 and 1980, probably related to a M = 5.0 earthquake in the vicinity. This traveltime drop could have been produced either by the closing of dry or saturated cracks in the crustal material or by the saturation of dry or partly saturated cracks. However, equal traveltime changes for both p- and s-waves, the depth-frequency distribution of microearthquakes and the anisotropy of traveltime changes in this area lead to the belief that this traveltime drop was caused by the closing of water saturated, aligned cracks in the crustal material underneath the St. Lawrence River. This would require a decrease in pore volume of the rocks and so lead to subsidence in this area. However, repeated levellings restrict the crustal motion to less than 2 cm. From this we conclude that the crustal region affected by the crack-closing process must be discontinuous. A possible model is one where the crack deformation occurs in isolated inclusions less than 1 km in diameter.

Résumé

Une baisse significative du temps de parcourt des ondes sismiques, jusqu'à 0.5%, s'est produite dans la région de Charlevoix entre les années 1979 et 1980, probablement relié à un séisme M - 5.0 dans la localité. Cette baisse du temps de parcourt aurait pu être produite soient par la fermeture de fissures sèches ou saturées du matériel de la croûte ou par la saturation de fissures sèches ou partiellement saturées. Cependant, des changements égaux de temps de parcourt pour les ondes S et P, la distribution de la fréquence des micro séismes en fonction de la profondeur et l'anisotropie des changements de temps de parcourt dans cette région porte à croire que cette baisse est causée par la fermeture de fissures saturées d'eau et allignées dans le matériel de la croûte sous le fleuve Saint-Laurent.

Ceci demanderait une diminution du volume des pores du rock et nous conduirait ainsi à un affaissement du sol dans cette région. Cependant, des nivellements répétés restraignent le mouvement de la croûte à moins de 2 cm. De tout ceci nous concluons que la croûte de la région affectée par le processus de fermeture de fissures doit être discontinuée. Un modèle possible est celui où la déformation des fissures se présente dans des inclusions isolées de moins d'un kilomètre de diamètre.

Introduction

Since 1974 the Charlevoix region in Quebec has been used as a geophysical testsite by the Earth Physics Branch in order to study intraplate seismic activity (Fig 1). During the investigation period changes in seismic traveltimes, magnetotelluric impedance, crustal uplift and gravity have been monitored regularly (Buchbinder, Kurtz and Lambert,1983). The region is mainly characterized by 2 geological features:

- the Paleozoic-Precambrian boundary striking nearly parallel to the northshore of the St Lawrence River and dipping at a low angle to the SE.
- and the Charlevoix impact structure centered about 5 km inland from the northshore and extending over a radius of about 20 km.

All microearthquakes in this region occur in the Precambrian rock underneath the St. Lawrence River; the Paleozoic-Precambrian boundary is shown to be inactive (Anglin and Buchbinder,1981; Fig. 2).
In August 1979 an M=5 earthquake occurred about 35 km north-east of the centre of the impact structure (Hasegawa and Wetmiller, 1980). At the same time a sudden drop in water head in a well at the Charlevoix observatory was observed, as well as a drop in impedance at one magnetotelluric station (Dufour). However, no significant changes were reported at the other MT-stations. In addition it is clear from gravity data and repeated levellings that no significant elevation changes in the Charlevoix region occurred at the time of the earthquake.
Calibration shots performed in the spring of 1980 showed a decrease in seismic traveltimes of about 0.5% (Fig. 3). This change, the largest traveltime change observed since 1974, may be associated with postseismic strain release affecting the cracks in the crustal material. In the following an attempt is made to interpret this traveltime decrease in terms of changes in crack properties within the crustal rocks in the Charlevoix region.

Microcracks in crustal rocks and their influence on seismic velocities

A microcrack is defined as "an opening that occurs in rocks and has one or two dimensions smaller than the third ... the length ... typically is of the order of 100 m or less" (Simmons and Richter, 1976). These microcracks are a very common feature in most crustal rocks. Parameters often used to describe microcracks are length, aspect-ratio (ratio of minor axis c to major axis a under the assumption of elliptical crack shape) and density (number of cracks per unit volume of rock). A useful combination of these

parameters is the crack density ε (O'Connell and Budiansky,1974) defined by

$$\varepsilon = N \langle a \rangle^3 \qquad (1)$$

where N = number of cracks per unit volume
and $\langle a \rangle$ = average crack length.

Crack density ε and aspect-ratio c/a are related to the porosity η by

$$\eta = \frac{4\pi}{3} \left(\frac{c}{a}\right) \varepsilon \qquad (2)$$

Typical values of crack lengths for granite are in the range of 1-50 μm (compiled by Kranz,1983). Typical values for aspect-ratios are in the range of 10^(-2) - 10^(-4) (Hadley,1976).
An increase in confining pressure tends to squeeze the cracks and to shift the aspect-ratio spectrum to lower values. The change in aspect-ratio is given by Walsh (1965) as

$$\partial\left(\frac{c}{a}\right)/\partial p = - \frac{4(1-\nu^2)}{\pi \cdot E} \qquad (3)$$

where P = confining pressure, E = Young's modulus
and ν = Poisson's ratio

A deviatoric stress component normal to the crack area tends to close the crack, (i.e. aspect ratio c/a→0), while a deviatoric stress parallel to its major axis tends to lengthen the crack, the width of it remaining roughly constant. Uniaxial deviatoric stress would, therefore, lead to an increase in crack-density and to a decrease in aspect-ratio of those cracks lying parallel to the stress direction, and no change in crack density but a decrease in aspect ratio for those cracks lying normal to the stress direction. In consequence this leads to anisotropy of rock under the influence of uniaxial deviatoric stress (extensive-dilatancy anisotropy, EDA, Crampin et al., 1984), as is shown in laboratory experiments (Nur and Simmons, 1969).
Seismic velocities of rocks are strongly affected by cracks. For a random orientation of flat "penny-shaped" cracks an algorithm by O'Connell and Budiansky (1974) can be used to calculate the resulting seismic velocities.

(4)

$$\frac{\bar{K}}{K} = 1 - \frac{16}{9}\left(\frac{1-\bar{\nu}^2}{1-2\bar{\nu}}\right)(1-\xi)\varepsilon$$

$$\frac{\bar{\mu}}{\mu} = 1 - \frac{32}{45}(1-\bar{\nu})\left[1 - \xi + \frac{3}{2-\bar{\nu}}\right]\varepsilon$$

$$\varepsilon = \frac{45}{16}\left(\frac{\nu-\bar{\nu}}{1-\bar{\nu}^2}\right) \cdot \frac{2-\bar{\nu}}{[(1-\xi)(1+3\nu)(2-\bar{\nu}) - 2(1-2\nu)]}$$

$$\frac{\bar{V}_p}{V_p} = \sqrt{\frac{(1-\bar{\nu})(1+\nu)}{(1+\bar{\nu})(1-\nu)} \frac{\bar{K}}{K}}$$

$$\frac{\bar{V}_s}{V_s} = \sqrt{\frac{\bar{\mu}}{\mu}}$$

$\bar{V}_p, \bar{V}_s$ seismic velocities of the crack bearing rock
$\bar{K}, \bar{\mu}, \bar{\nu}$ elastic properties of the crack bearing rock
K, μ, ν elastic properties of the rock matrix
ξ water saturation degree $\xi = 0.....1$

The well-known results are shown in Fig.4. However this theory does not include changes in aspect ratio of the cracks. To take aspect ratio into account the algorithm was modified (O'Connell and Budiansky,1974) by

introducing a new parameter ω depending on the aspect ratio of the cracks and on the bulk moduli of pore fluid and crack-free rock. The system of equations to be solved is now

(5)

$$\frac{\bar{K}}{K} = 1 - \frac{16}{9}\frac{(1-\bar{\nu}^2)}{(1-2\bar{\nu})} D\,\varepsilon$$

$$\frac{\bar{\mu}}{\mu} = 1 - \frac{32}{45}(1-\bar{\nu})\left[D + \frac{3}{2-\bar{\nu}}\right]\varepsilon$$

$$\varepsilon = \frac{45}{16}\frac{(\nu-\bar{\nu})}{(1-\bar{\nu}^2)} \cdot \frac{2-\bar{\nu}}{[D(1+3\nu)(2-\bar{\nu}) - 2(1-2\nu)]}$$

$$D = \left[1 + \frac{4}{3\pi}\frac{(1-\bar{\nu}^2)}{(1-2\bar{\nu})}\frac{K}{\bar{K}}\omega\right]^{-1}$$

$$\omega = \frac{a}{c}\frac{\tilde{K}}{K}$$

$\tilde{K}$ = bulk modulus of pore fluid

The results for cracks filled with water ($\tilde{k}$=23 kbar) are shown in Fig.5.

Aligned cracks in rock produce an anisotropic velocity distribution. This can be calculated using Crampin's (1978) formulae

$$\bar{V}_p(\cos\Theta) = V_p \Big/ \left[(1-\xi)/R^D + \xi/R^S\right] \qquad (6)$$

$$R^D = \sqrt{1 - \frac{11}{21}\varepsilon - \frac{8}{3}\varepsilon\cos 2\Theta + \frac{\varepsilon}{21}\cos 4\Theta}$$

$$R^S = \sqrt{1 - \frac{8}{21}\varepsilon + \frac{8}{21}\varepsilon\cos 4\Theta}$$

where Θ = angle between raypath and crack normal

In this use the cracks are considered as flat and "penny-shaped" so that the aspect ratio is close to zero. P-wave velocities as a function of azimuth are shown in Fig.6.
However, this is only valid for vertical cracks. For the case of cracks dipping by an angle β (normal to the crack with respect to the horizontal) the angle Θ in (6) must be replaced by $\arccos(\cos\theta\cos\beta)$ (Grenier, 1984). Anisotropy of p-wave velocities caused by water saturated aligned and dipping cracks are shown in Fig. 7a. In the case of "extensive-dilatancy-anisotropy" cracks aligned in the direction of uniaxial stress can still be dipping in a random manner, in an azimuth normal to the direction of the external stress. The resultant anisotropy of p-wave velocities with azimuth is calculated by averaging over all dip angles . This is shown in Fig 7b. Results for the aligned and the randomly oriented system can be linked by superposition of several aligned crack systems. A quasi-random oriented crack system consisting of 6 superimposed aligned systems shifted by 30° was in agreement within 10 % with the corresponding random oriented system calculated after O'Connell and Budiansky (1974).

Discrimination between dry and saturated cracks.

Seismic travel-time changes in rocks as shown in Fig. 4 can be caused either

by changes in crack density or by changes in saturation degree of the cracks. It is important to discriminate between these cases because a travel-time change caused by a change in saturation degree would not be accompanied by a change in porosity of the rock. So for this case no vertical movement could be expected. Some evidence exists that the reported travel-time drop in the Charlevoix region between 1979 and 1980 was caused by the closing of saturated cracks. In the following the facts leading to this assumption will be discussed.

A) Equivalence of p- and s-wave traveltime changes.

Buchbinder (1981) reported roughly the same travel-time changes for both p- and s-waves in the Charlevoix region for the period 1974-1979. The same statement can be made for the period of 1979 up to now. However s-wave arrivals can only be observed for shots detonated and recorded on the northshore of the St. Lawrence River because s-waves are strongly scattered by the Paleozoic rocks underneath the St. Lawrence. So the following is valid only for the north shore region. The conditions of the rocks underneath the St. Lawrence River might be different.
From Fig. 4 it is clear that an increase in seismic velocities for both p- and s-waves can be obtained either by saturating dry cracks or by decreasing the crack density ε . This would lead to a change in traveltime defined by

$$t' = t + \Delta t \qquad t'/t = v/v' \tag{7}$$

$$\Delta t/t = v/v' - 1$$

This traveltime change can be caused either by a change in water saturation or a change in crack density. To distinguish between these cases we calculate the derivatives with respect to ε and ξ .

$$\partial(\Delta t/t)/\partial\varepsilon = \partial(v/v')/\partial\varepsilon \qquad \partial(\Delta t/t)/\partial\xi = \partial(v/v')/\partial\xi \tag{8}$$

The right hand side of both equations is given by O'Connell and Budiansky's formulas (1974). However due to the complexity of their system of equations the derivatives cannot be calculated in a straightforward manner unless a simplification is made. From Fig. 4 it is obvious that the effective Poisson's ratio of cracked rock is nearly a linear function of the crack density ε and can be expressed as

$$\bar{\nu} = \nu + p(\xi)\cdot\varepsilon \tag{9}$$

The gradient $p(\xi)$ can be calculated using equations (19) and (20) of O'Connell and Budiansky (1974) for the endpoints of the $\bar{\nu}-\varepsilon$ curves. After substituting (9) into the expression for the effective bulk- and shear-moduli the derivatives can then be calculated in a straightforward manner. For the comparison of traveltime changes for p- and s-waves it must be remembered that traveltimes for s-waves are normally $\sqrt{3}$ times longer than for p-waves, so that relative changes in p-wave velocities $\Delta\bar{V}_P/\bar{V}_P$ must be greater than relative changes in s-wave velocities $\Delta\bar{V}_S/\bar{V}_S$ by the same factor to get equivalent travel-time changes.
The calculated traveltime changes due to changes either in crack density or in water saturation are shown in Fig. 8. For changes in crack density we get similar traveltime changes for p- and s-waves only for nearly saturated

cracks, while for traveltime changes due to changes in water saturation we get this result either for dry cracks at moderate (ε=0.1) crack density or for semi saturated cracks at high (ε=0.4) crack density. So, under the assumption of a reasonable crack density the cracks prior to the travel-time drop must be either completely dry or completely saturated, intermediate cases would require a high crack density. These arguments apply to the case where the cracks in the crater region are randomly oriented.

B) The depth-frequency distribution of earthquakes in the Charlevoix region.

From 1978 to 1982 a total of 399 earthquakes covering the magnitude interval from M=-0.7 to M=5.0 were recorded by the seismometer array installed in the Charlevoix region. From these 379 earthquakes were chosen for examination of their depth-frequency distribution. For the remaining earthquakes either no focal depth could be determined or they were located far from the impact structure.
From Fig 2 it is obvious that the hypocenters are clustered into two groups, one underneath the Paleozoic sediments along the southshore and one along the northshore without a Paleozioc overburden. The depth-frequency distribution of both groups (Fig 9) exhibits no striking differences with the exception that no earthquakes occur within the Palezoic sediments and so the peak at a focal depth of 5 km for the northshore earthquakes is missing in the southshore depth-frequency distribution.
Combining both regions leads to a depth-frequency distribution for the entire Charlevoix region (Fig 10). This distribution is characterised by two distinctive peaks at depths of 10 and 18 km. After Meissner and Strehlau (1982) the peak depth in the depth-frequency distribution is identical with the depth where the crustal material has its maximal strength. This strength-depth distribution depends on the crustal heat flow; different distributions exist for both dry and wet crustal material. The maximal strength for dry material is at greater depth than for wet material. This gives an opportunity to distinguish between dry and saturated crustal material.
From Fig 3 (a and b) of Meissner and Strehlau (1982) we obtain the depth-strength distribution for both dry and wet material for heat flow of 1.5 HFU and 1.4 HFU, the latter by interpolation (Fig 10). The peak in the depth - frequency distribution of microearthquakes at a depth of 10 km is nearly identical with the peak in the depth-strength distribution for wet crustal material at a heat flow of 1.5 HFU, while the second peak at a depth of 18 km refers to dry crustal material. From this we can conclude that at least the upper 10 km of the crust in the Charlevoix region is wet, so that existing cracks in the crustal material up to that depth should be water-saturated.
No heat flow measurements have been made in the Charlevoix region. The average heat flow for the Grenville Province is 1.11 HFU (Jessop et al, 1984). However, values up to 1.32 HFU were measured so that an assumed value of 1.5 HFU for the Charlevoix region seems to be reasonable.

Equal travel-time changes for p- and s-waves can be obtained either for dry or for saturated crustal material. However, dry crustal material would have its maximal strength at a greater depth than the 10 km as indicated by the peak distribution of microearthquakes. So we conclude that the crustal material in the Charlevoix region including its pores and cracks is water saturated.

Traveltime and uplift changes for randomly oriented cracks.

As is obvious from Fig. 4, the required velocity increase of 0.5% for the time interval 1979-1980 can be obtained easily by saturating dry cracks. In this case the pore volume would remain unchanged, and so no vertical movement would occur.
But as was shown in the previous section, closing of saturated cracks is more likely. In that case the conditions are more complicated. Let us assume the cracks would close in the same manner as they would open under the influence of uniaxial stress, i.e. shortening with constant crack width with the consequence of an increase in aspect ratio.
Under the assumption that crack aspect ratios are 10^(-3) or less and that the cracks are water saturated, the change in aspect-ratio accompanying a change in crack density (crack lengthening/shortening model) will have a minor effect (Fig. 5) and equations (4) can be used to calculate the resulting velocity changes (Fig. 11). The aspect-ratio scale in the upper part of this figure is nonlinear because of the cubic dependence of the crack density on crack length. So for an arbitrarily chosen starting point in 1979 with crack density $\varepsilon = 0.05$ and aspect ratio 3*10^(-3) an increase in p-wave velocity of 0.5% is obtained by a transition to a crack density of 0.03 and an aspect-ratio of 3.6*10^(-3). Using (2) this corresponds to a decrease in rock porosity from 0.63*10^(-3) in 1979 to 0.45*10^(-3) in 1980.
This decrease in pore volume would lead to subsidence of the surface above the crack-bearing region. The vertical ground motion caused by a buried dilating or collapsing sphere can be calculated by

$$\Delta h = \frac{2(\lambda+2\mu)}{\lambda+\mu} a^2 \Delta a \frac{h}{(x^2+h^2)^{3/2}} \qquad (10)$$

(Hagiwara, 1977, for notation see Fig.12)
The zone of microearthquake activity in the Precambrian rock underneath the St. Lawrence River, in which the velocity changes occur (Fig. 2), can be approximated by a sphere of 12 km radius beneath a 3 km thick layer of overburden. Under the assumption that the entire sphere is affected by the velocity changes and that crack density as well as aspect-ratio of the cracks are uniform over the sphere, the required change in porosity would lead to a decrease in radius of about 0.7 m. From this we can calculate a subsidence of about 1.2 m above the centre of the sphere (i.s. the middle of the St. Lawrence River) and of about 0.5 m on the north shore. That is approximately the location where repeated levellings have been carried out and where no significant change in elevation between 1978 and 1980 occurred.

The absence of vertical motion provides strong constraints for the parameters used in this model. The predicted subsidence can be reduced by decreasing the crack aspect-ratio and/or the size of the crack-bearing region. The change in radius of the crack-bearing sphere is related to the crack porosities in 1979 and 1980 by

$$\Delta a = a \left[\left(\frac{1-\eta_{79}}{1-\eta_{80}} \right)^{3/2} - 1 \right] \qquad (11)$$

These porosities are small compared to unity and so a linear relationship exists between aspect-ratio and the change in radius of the crack-bearing sphere. On the other hand, from Fig. 5 it is clear that for small aspect-ratios (<10^-3) the seismic velocities are roughly independent of the aspect-

ratio. In other words for c/a = 10^(-3) changes in aspect-ratio do not affect the seismic velocity but the mean value of aspect-ratio in the stressed region is an important factor in the determination of associated vertical movement. Some limits can be placed on that by the following arguments: A crack aspect-ratio of 10^(-3) is roughly the average value for igneous surface rocks. At greater depths however the cracks will be squeezed and the aspect-ratio distribution will shift to lower values following the previously mentioned formula by Walsh (1965). Thus, for example, a rock showing a surface aspect-ratio distribution centered at 5*10^(-3) will have a mean aspect ratio of 4*10^(-3) at a depth of 3 km.
The choice of a crack-bearing zone that coincides with the entire seismically active region was arbitrary and the adoption of the spherical shape for the zone was done for computational simplicity. The ray-paths of the seismic experiment penetrate only the uppermost part (4 km) of the microseismic region. Therefore, the zone where a change in crack volume occurs and uplift or subsidence is produced might be much smaller than the microseismic region.
Taking both of these factors into account we calculated the subsidence produced by some subspheres of the microseismic region under the two assumptions:(Fig. 13)

- the upper boundary of the subsphere shall be given by the upper boundary of the microseismic region (3 km).
- the crack aspect-ratio at the lower boundary of the subsphere shall be zero. Using the aspect-ratio vs depth diagram after Walsh (1965) we take the resulting aspect ratio at the centre of the subsphere as the average aspect ratio of the cracks in the subsphere.

As a result we obtain that a sphere with a radius of only 2 km would produce subsidence within the error range of the levellings (here taken as 2 cm). This is the uppermost boundary of the radius of the subsphere, because the seismic raypath within the sphere is only a fraction of the entire raypath and so changes in crack density within the sphere must be higher than when averaged over the entire raypath. The vertical motion is proportional to a^3 (a=radius of the crack-bearing sphere) for a given change in crack porosity η but $\Delta\eta$ required to fit the traveltime data is proportinal to 1/a (smaller sphere needs larger change of porosity). The vertical motion produced by a spherical inclusion is therefore proportional to a^2 . So the radius of the sphere causing vertical motion within the error range of the levellings is about 1 km, but the required changes in crack density are very high, roughly 0.4.

Traveltime and uplift changes for aligned cracks.

In search for evidence of aligned cracks the travel-time ratios 79/60 for all seismometer sites are plotted against the azimuths of the raypaths (Fig. 14). The shot points, seismometer sites and the definition of azimuths are given in Fig. 15. From Fig. 14 no azimuthal dependence of travel-time ratios is obvious. However, the seismic waves have to penetrate 3 different geologic materials, Paleozoic sediments on the southshore and underneath the St. Lawrence River (Vp=5.8 km/s), Precambrian granitic gneiss on the northshore (Vp=6.0 km/s) and an anorthosite body farther to the north (Vp=6.4 km/s). So this variety of seismic velocities may obscure any azimuthal dependence of traveltime changes.
To avoid this problem only seismometer sites whose raypaths had to cross the St. Lawrence River were chosen for comparison. In addition, a correction

for the deflection of the raypath at the Paleozoic-Precambrian boundary underneath the St. Lawrence River was applied. This correction has a significant value only for seismometer stations with long shotpoint distances, so for example a correction of -6.0° has to be applied for station 64, -4.7° for station 62 and -3.0° for station 60.
The results are shown in Fig. 16, it is obvious that with 2 exceptions all stations can be fitted with a theoretical curve for aligned watersaturated cracks (Crampin,1978). Both exceptions, station 16 and station 58, are located close to the Charlevoix impact structure and may be affected by a local fracture system restricted to the crater area. The data cannot be fitted under the assumption of dry or partly saturated cracks (Fig. 17). This is evidence that the travel-time changes '79-'80 are caused by a decrease in crack density for saturated cracks.
The fit can only be done under the assumption of vertical aligned cracks. Randomly dipping cracks, although in accordance with the EDA-theory as mentioned before, would produce a different pattern of travel-time anisotropy and so can be ruled out (Fig. 18).
The assumption of a local fracture system inside the crater area is backed by the fact that the same fit of traveltime data with a theoretical curve can be done for shots whose raypaths had to cross the crater region (shotpoints and seismometer sites on the northshore). In this case the reference system for crack directions has to be shifted by 18° ;that means the assumed cracks are running in ENE-WSW direction (Fig. 19).
The traveltime data can be fitted either by the transition from aligned cracks at $\varepsilon = 0.05$ to aligned cracks at $\varepsilon = 0.015$ or by the transition from aligned cracks at $\varepsilon = 0.06$ to randomly oriented cracks at $\varepsilon = 0.03$. We cannot distinguish between these cases because after 1980 the traveltime changes are too small to detect any anisotropy.
The direction of the aligned crack system cannot be deduced from the travel-time data in an unequivocal manner. Two perpendicular crack systems are possible, oriented roughly either in a NS or in an EW direction.
In order to calculate uplift or subsidence created by opening or closing aligned cracks we assume that a crack opens or closes in a direction perpendicular to the plane defined by its larger semi-axis. This is in accordance with the assumptions of the extensive-dilatancy model (Crampin et al, 1984).In the following the calculation procedure is explained in terms of opening cracks; however, for the case of closing cracks one has only to change the sign. The opening of a crack creates a displacement field in the surrounding material. This can be calculated under the assumption that the opening crack can be replaced by the superposition of double forces without moment in the direction of the opening (Fig. 20). Such a double force without moment can be represented by a Galerkin vector defined by (12)

$$G_x^x = \frac{2x}{R} - \frac{4(1-D)(1-2D)}{R+c} + \frac{2c^2x}{R^3}$$

$$G_y^x = 0$$

$$G_z^x = \frac{2c}{R} - \frac{2cx^2}{R^3} + \frac{2(1-2D)x^2}{R(R+c)} + 2(1-2D)\log(R+c)$$

for double forces without moment in the x-direction

$$G_x^y = 0$$

$$G_y^y = \frac{2y}{R} - \frac{4(1-D)(1-2D)y}{R+c} + \frac{2c^2y}{R^3}$$

$$G_z^y = \frac{2c}{R} - \frac{2cy^2}{R^3} + \frac{2(1-2D)y^2}{R(R+c)} + 2(1-2D)\log(R+c)$$

for double forces without moment in the y-direction

$$G_x^z = 0$$

$$G_y^z = 0$$

$$G_z^z = -\frac{4Dc}{R} + 4D(1-2D)\log(R+c)$$

for double forces without moment in the z-direction (vertical)
where $R = x^2 + y^2 + c^2$ and $c =$ depth of crack below the surface (Mindlin and Cheng, 1950).
The displacement field for a given point at the free surface can be calculated by the partial derivatives of the Galerkin vector, for the special case of vertical motion (13)

$$u_z = \frac{1}{2\mu}\left[2(1-D)\,\Delta G_z - \frac{d}{dz}\,\mathrm{div}\,G\right]$$ (Mindlin and Cheng, 1950)

For cracks opening parallel to one axis of the coordinate system the resulting uplift can now be calculated directly, for the case of dipping cracks the corresponding Galerkin vector is a superposition of elemental Galerkin vectors with and without moment following the formula for tensor rotation (14)

$$G_i^x(\alpha) = G_i^x \cos^2\alpha + G_i^z \sin^2\alpha + 2\,G_i^{xz} \sin\alpha\cos\alpha$$

$$G_i^z(\alpha) = G_i^x \sin^2\alpha + G_i^z \cos^2\alpha - 2\,G_i^{xz} \sin\alpha\cos\alpha$$

$$G_i^y(\alpha) = G_i^y \qquad i = x, y, z$$

The Galerkin vectors with moment are also given by Mindlin and Cheng (1950). The resulting vertical motion for a spherical region bearing cracks is shown in Fig. 21. It is obtained by numerical integration over the Galerkin vectors of this volume. However, these results are only qualitative. Neither the magnitude of the single Galerkin vector nor the crack density were taken into account. The results can, however, be normalized by the corresponding case of random crack orientation by averaging over several crack directions as shown in Fig. 21. The vertical motion for aligned vertical cracks extending or contracting parallel to the direction of the profile can also be compared to the result for randomly oriented cracks (Fig. 22). From these results it can be stated that compared to the case of random orientation, aligned vertical cracks produce half as much vertical motion at the location of the levelling line. If the cracks are oriented NS or EW, the vertical motion will change from uplift to subsidence along the NE-SW striking levelling line.
From the calculated vertical motion for a sphere filled with randomly oriented cracks in which the crack density decreases from 0.06 in 1979 to 0.03 in 1980 and the results of Figs. 21 and 22 we obtain a change from +20

cm to -20 cm along the levelling line where no vertical motion has been recorded. Again, even for the case of aligned cracks the volume of the crack-bearing crustal region has to be reduced radically to obtain vertical motion well within the error range of the repeated levellings.

The multiple inclusion model for extensive dilatancy anisotropy

A single inclusion with a radius not exceding 1 km can explain the lack of vertical crustal motion in connection with the traveltime event. However, this model requires the assumption of very large changes in crack density within the inclusion. Moreover, a single spherical inclusion would not affect all raypaths of the seismic experiment. It would have to be replaced by a crack-bearing elongated ellipsoid or cylinder in the Precambrian rock underneath the St. Lawrence River. To avoid these unlikely assumptions we postulate a model containing a pattern of small crustal inclusions bearing aligned watersaturated cracks (Fig. 23). The mean depth of these inclusions must be 4 km beneath the St. Lawrence River to affect the seismic rays. It must be shallower beneath the crater region because the raypaths do not penetrate as deeply there as a result of shorter shotpoint distances. For such a pattern of inclusions at a depth of 4 km and with a 3 km inclusion spacing, the dependence of vertical motion on the radius of the inclusion has been calculated (Fig. 24). As a result we get that inclusions with a radius not exceeding 400 m would produce vertical motion below the previously mentioned error range. Here the correction for the fractional length of the ray-path has been applied already. The assumed crack aspect-ratio is 10^(-3).

Discussion and Conclusions.

The traveltime drop '79 - '80 can be produced either by saturating under-saturated cracks in the rock or by decreasing the crack density for saturated cracks. The equivalence of p- and s-wave travel-time changes around the time of the '79 - '80 event restricts the crack behaviour to two possibilities: either closing of saturated or nearly saturated cracks or resaturating of dry or semi-filled cracks, the latter case requires a high crack density. There is some support for the crack-saturation case: a sudden water-table drop in wells close to the Charlevoix observatory at the time of the '79 earthquake, a decrease in impedance at the magnetotelluric station Dufour (DUF, Fig.1) contemporary to the earthquake, and the presence of a steeply dipping fracture system acting as a boundary in seismicity (Anglin and Buchbinder, 1981) which might feed the cracks in the Precambrian rock underneath the St. Lawrence River with water. Also, the time delay between the earthquake and the subsequent travel-time drop (calibration shots detonated a few weeks after the earthquake showed no change in travel-time) indicates that the travel-time drop might be related to water diffusion. However, the frequency-depth distribution of microearthquakes in this region leads to the belief that at least the upper 10 km of the crust are "wet" and so that the existence of dry cracks prior to the travel-time drop seems to be unlikely. Moreover, the anisotropic pattern of traveltime changes vs raypath azimuth indicates clearly that the traveltime changes are caused by changes in crack density for saturated rocks. Even a transition from nearly saturated (ξ =.95) to saturated (ξ =1.00) cracks would produce a totally different pattern of anisotropy and

can so be ruled out. The anisotropic pattern of traveltime changes can be created by two perpendi- cular crack systems (Fig 23) underneath the St. Lawrence River, one running roughly in a NS-direction and one running roughly in an EW-direction. The general direction of tectonic stress in this region is roughly in an EW-direction (Hasegawa and Wetmiller,1980; Hasegawa and Adams,1981) so that during the stress build-up phase prior to the '79 earthquake a hypothetical crack system in a NS-direction would be closed and so can be ruled out as a creator of the traveltime changes. However, following the theory of extensive-dilatancy anisotropy (Crampin et al.,1984) the crack system running in an EW-direction could be opened at this time and could produce the observed anisotropy.
The empirical relationship between the magnitude of an earthquake and the characteristic radius of the region affected by forerunner phenomena

$$\log L = 0.26\ M + 0.46$$ (Anderson and Whitcomb,1975)

gives a radius of the affected zone of about 50 km for a M=5 earthquake. The epicentral distance to the center of the Charlevoix impact structure is about 40 km, so that this region might well be affected by stress-related phenomena related to this earthquake.
After the earthquake,on the average, stress-release occurred. In consequence, the opened crack system closed again so that the cracks in the crustal material underneath the St.Lawrence River became either randomly oriented or aligned, but with a lower crack density. The time delay between the earthquake and the closure of the oriented crack system indicates that this process is anelastic in nature.
The closing process requires a decrease in pore volume. Under the assumption that the entire microseismic region approximated by a sphere underneath the St. Lawrence River is affected by this crack closure, an uplift of 20 cm is obtained at the north shore of the river. However, repeated levelling in this region indicates that no significant vertical crustal motion (>2 cm) occured between 1970 and 1980. This gives rise to a radical restriction on the size of the crack-bearing zone. Only a sphere with a radius of 2 km or less would lead to vertical motion within the error range of the levellings (2 cm). However, after a correction is applied for the fraction of the seismic raypath affected by this sphere the radius of the sphere is reduced to 1 km and very high changes in crack density are required.
An alternative model consists of small inclusions bearing cracks underneath the St.Lawrence River and underneath the crater region (Fig. 25). For the pattern of inclusions underneath the St. Lawrence River a model consisting of spheres with a radius a 400 m, a mean depth of 4 km and a centre-distance of 3 km would produce vertical motion within the error range of the levellings. In this model the changes in crack density are the same as used to fit the traveltime changes, the crack aspect-ratio is assumed to be 10^(-3). Within the crater region the inclusions must be shallower to affect the shallower raypaths, therefore their radius must be smaller. The crack system assumed to fit the traveltime data for the crater region is shifted by 18 with respect to the assumed crack system underneath the St. Lawrence River. This can be explained by a possible deflection of the general tectonic stress field by the impact structure. Whereas the inferences on applied stress directions are dependent on the existence of an azimuthal dependence of traveltimes, the requirement that the source of seismic travel-time changes be discontinuous is not.

Acknowledgements

R. K. was supported by an NSERC Visiting Fellowship held at the Earth Physics Branch. The authors are grateful to P. Grenier for writing the program for the velocity modelling. F. Anglin supplied the earthquake data file. We thank D. Bower, A. Goodacre, R. Kurtz, M. Paul and B. Robertson for helpful discussions and M.R. Dence for suggesting improvements to the manuscript.

References

Anderson, D.L. and J.H. Whitcomb: Time-Dependent Seismology. J. Geophys. Res. Vol. 80, 1497-1503, 1975.

Anglin, F. and G. Buchbinder: Microseismicity in the Mid St. Lawrence Valley Charlevoix Zone, Quebec. BSSA, Vol.71, No.5, 1553-1560, 1981.

Buchbinder, G.G.R.: Precise P and S Wave Velocity Variations, Crack Density, and Saturation Changes. J. Geophys. Res. Vol. 86, 1042-1046, 1981.

Buchbinder, G.G.R., R.D. Kurtz and A. Lambert: A Review of Time-Dependent Geophysical Parameters in the Charlevoix Region, Quebec. Earthq. Predict. Res., 2, 149-166, 1983.

Crampin, S.: Seismic-wave propagation through a cracked solid: polarization as a possible dilatancy diagnostic. Geophys. J. R. astr. Soc. 53, 467-496, 1978.

Crampin, S., R. McGonigle and D.Bamford: Estimation of crack parameters from observations of p-wave velocity anisotropy. Geophysics, 45, 345-360,1980.

Crampin, S., R. Evans and B.K. Atkinson: Earthquake Prediction: a new physical basis. Geophys. J. R. astr. Soc. 76, 147-156, 1984.

Grenier, P.: Variations de la Vitesse dans un Roc Fracture. Internal report 5/1984, Division of Seismology and Geomagnetism, Earth Physics Branch, Department of Energy Mines and Resources, Ottawa, Ontario, 1984.

Hadley, K.: Comparison of Calculated and Observed Crack Densities and Seismic Velocities in Westerly Granite. J. Geophys. Res. Vol. 81 3484-3494, 1976.

Hagiwara, Y.: The Mogi Model as a Possible Cause of the Crustal Uplift in the Eastern Part of Izu Peninsula and the Related Gravity Changes Bulletin of the Earthquake Research Institute, Tokyo University, 1977 (in Japanese), English translation by: Multilingual Services Division, Translation Bureau, Secretary of State, Canada.

Hasegawa, H.S., R.J. Wetmiller: The Charlevoix Earthquake of 19 August 1979 and its seismotectonic enviroment. Earthquake Notes, 51, 23-37, 1980.

Hasegawa, H.S., J. Adams: Crustal Stresses and Seismotectonics in Eastern Canada. Earth Physics Branch Open File No 81-12, 1981.

Jessop, A.M., T.J. Lewis, T.J. Judge, A.S. Taylor and Drury, M.J.: Terrestrial Heat Flow in Canada. Tectonophysics, 103: 239-261, 1984.

Kranz, R.L.: Microcracks in Rocks: a Review. Tectonophysics, 100 , 449-480, 1983.

Nur, A., and G. Simmons: Stress-induced velocity anisotropy in rock: an experimental study. J. Geophys. Res. 74, 6667-6674, 1969.

Meissner, R., and J. Strehlau: Limits of Stresses in Continental Crusts and their Relation to the Depth-Frequency Distribution of Shallow Earthquakes Tectonics 1, 73 - 89, 1982.

Mindlin, R.D., and D.H. Cheng: Nuclei of Strain in the Semi-Infinite Solid. Journal of Applied Physics, 926-930, 1950.

O'Connell, R.J., and B. Budiansky: Seismic Velocities in Dry and Saturated Cracked Solids. J. Geophys. Res. 79, 5412-5426, 1974.

Simmons, G., and D. Richter: Microcracks in Rock. In: R.G.J. Strens (Ed.), The Physics and Chemistry of Minerals and Rocks, Wiley, New York, 105-137, 1976.

Walsh, J.B.: The Effect of Cracks on the Compressibility of Rock. J. Geophys. Res.,70, 381-389, 1965.

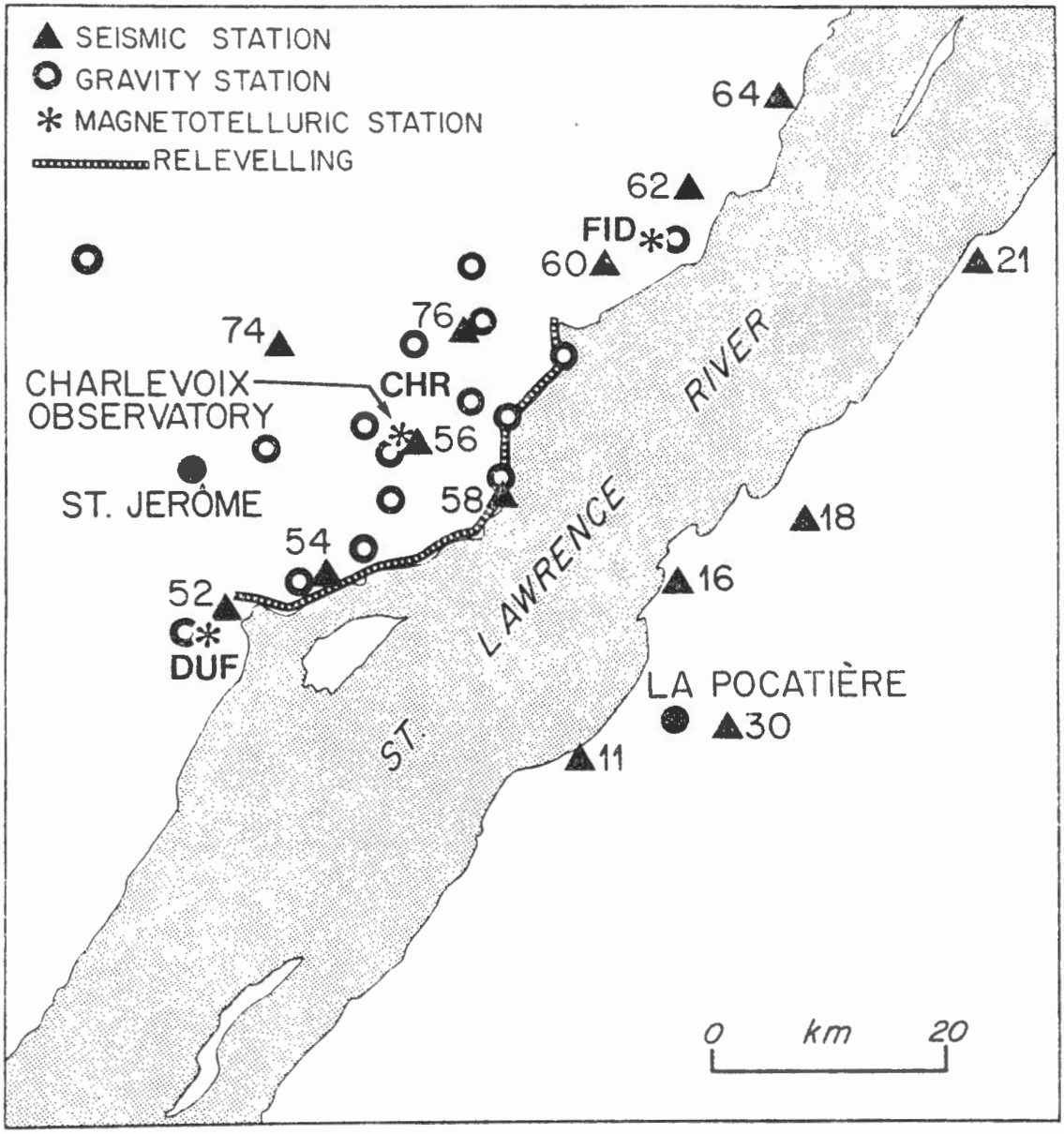

Fig. 1 Seismic, gravity and magnetotelluric stations and the levelling line at the Charlevoix geophysical testsite.

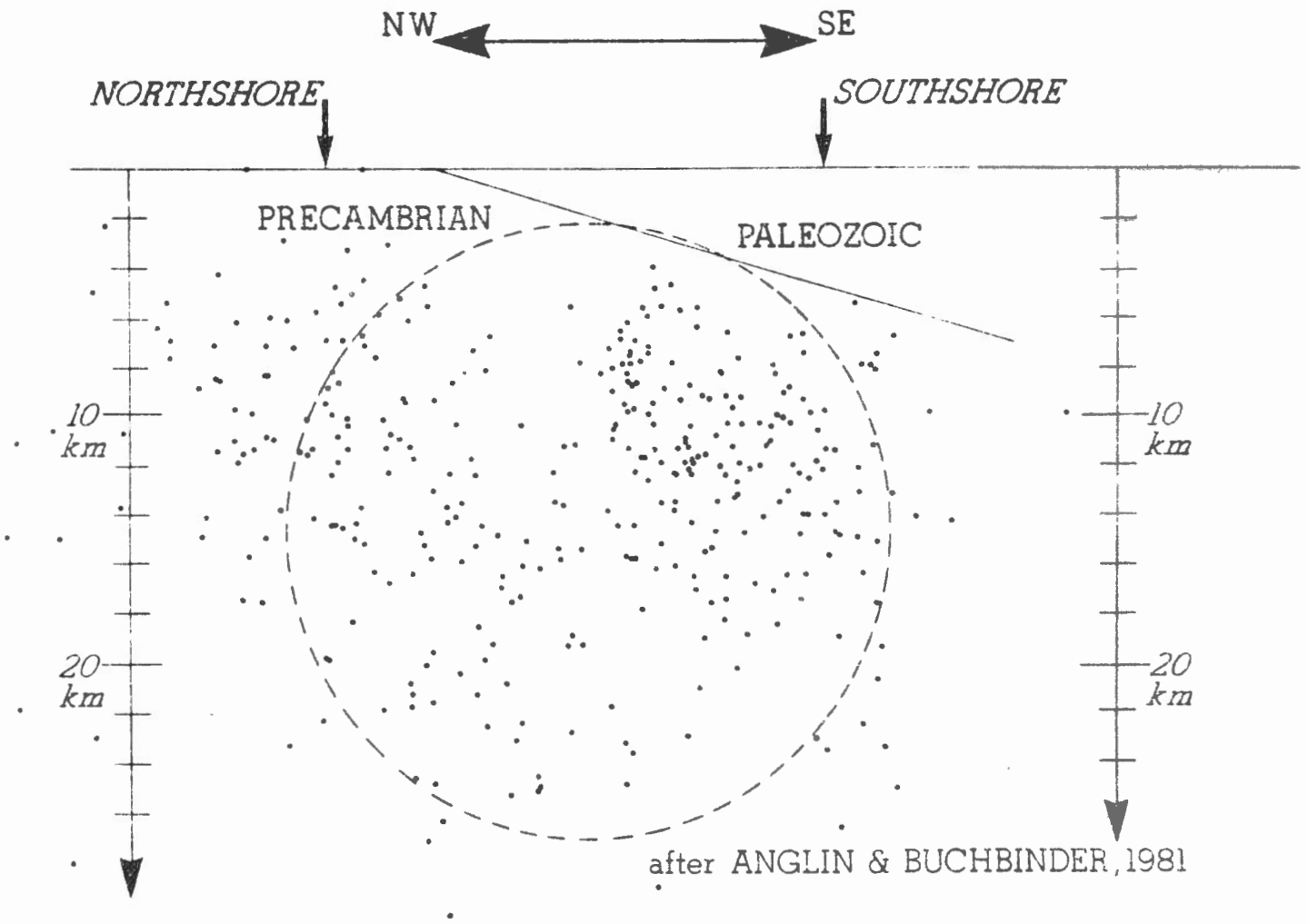

Fig. 2 Crosssection of the microseismic foci in the Charlevoix area

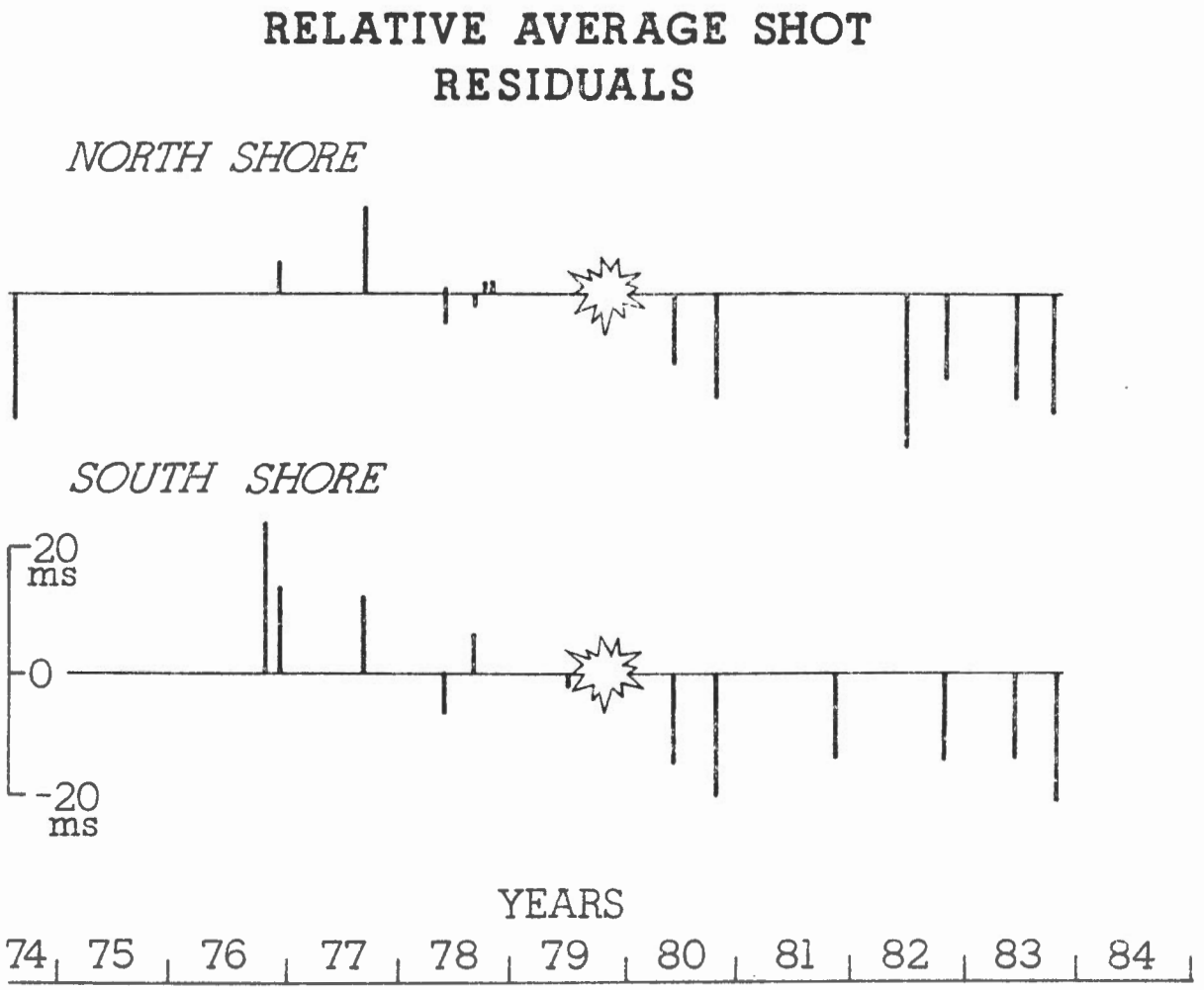

Fig. 3 Relative average seismic traveltime residuals for the Charlevoix experiment.

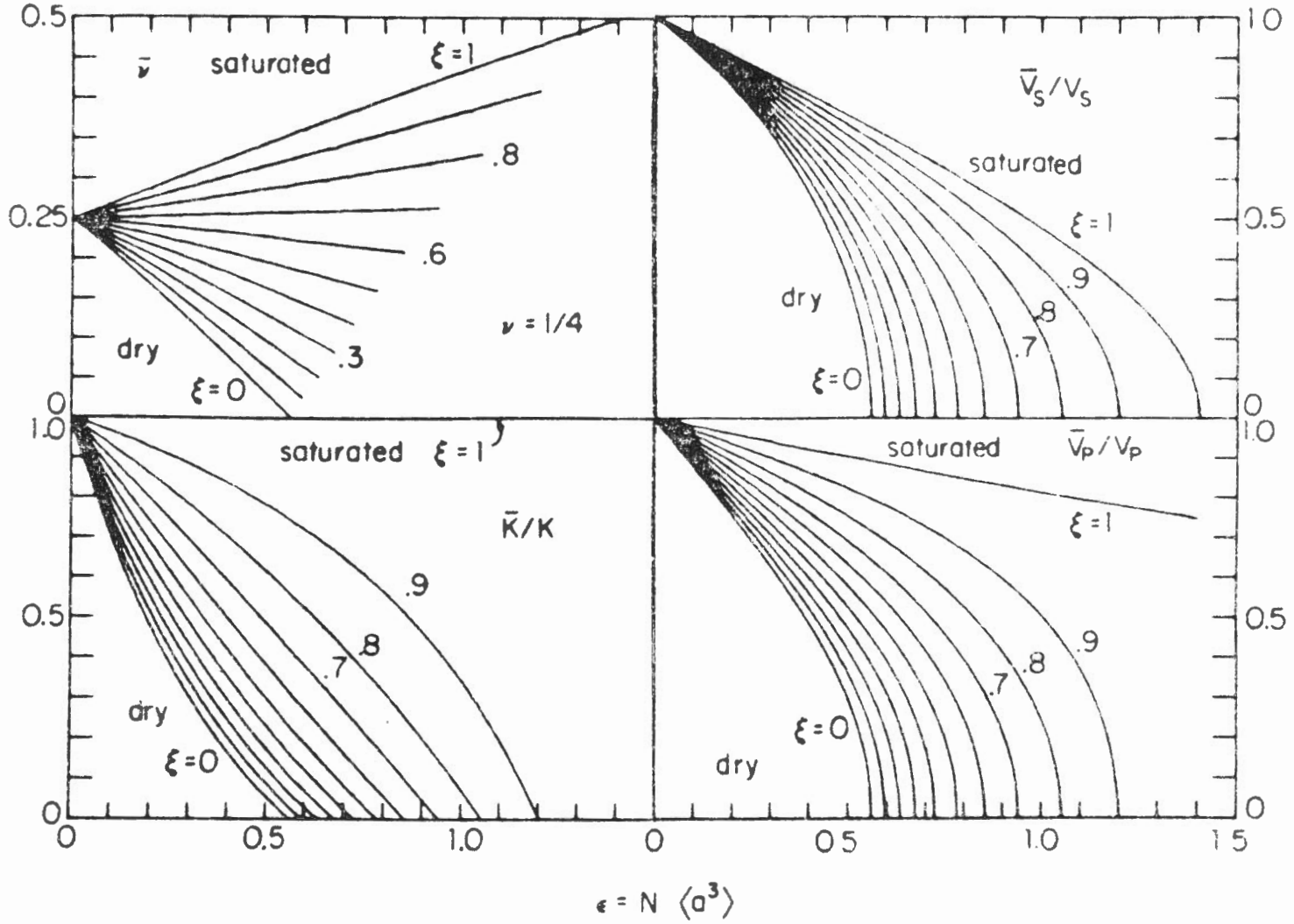

Fig. 4 Elastic parameters and seismic velocities for cracked rock after O'Connell and Budiansky (1974). See text for definition of parameters.

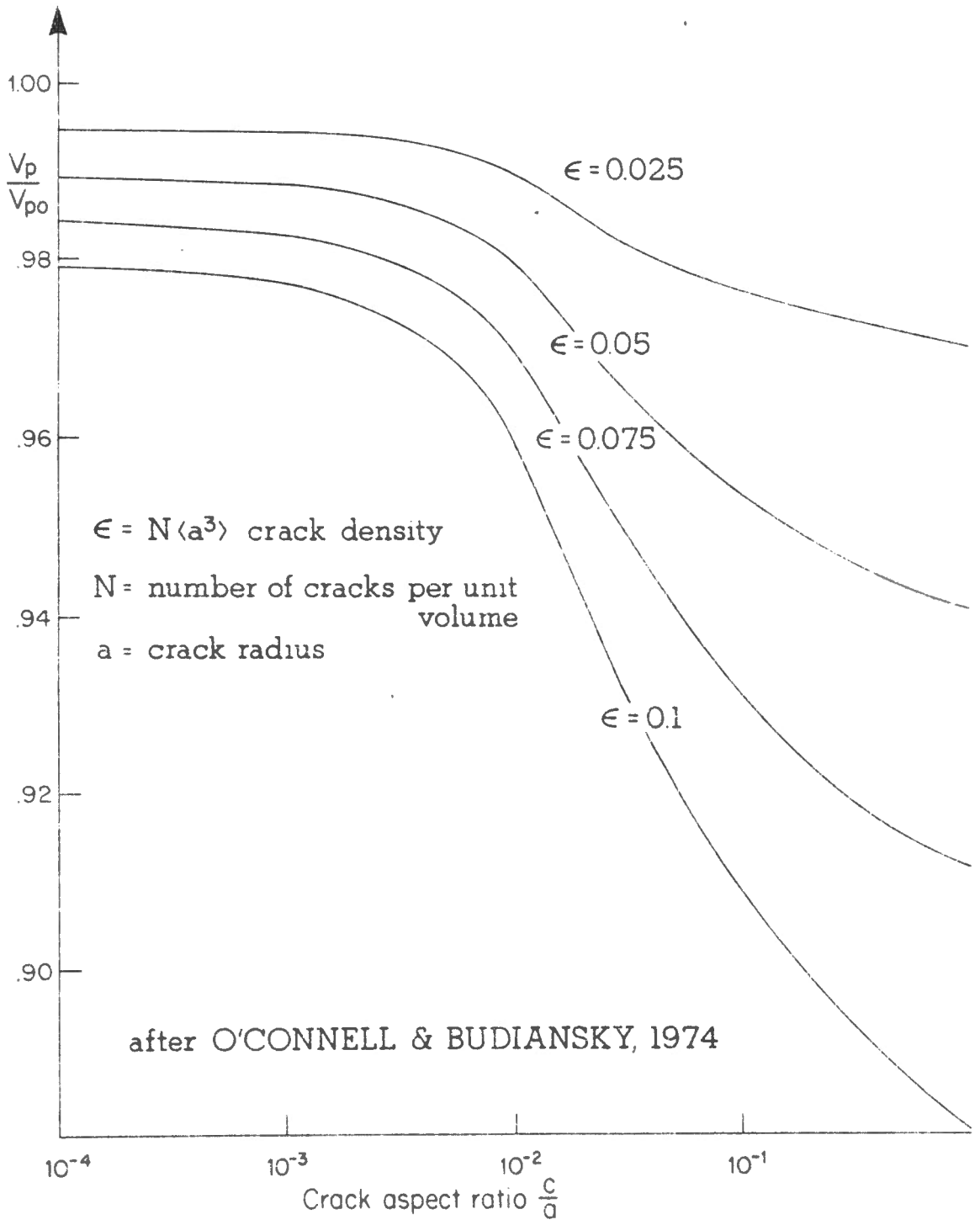

Fig. 5 Seismic velocities for cracked rock under the assumption of constant bulk modulus of the pore fluid (computed after O'Connell and Budiansky, 1974). Vp_o is the seismic velocity of the rock matrix.

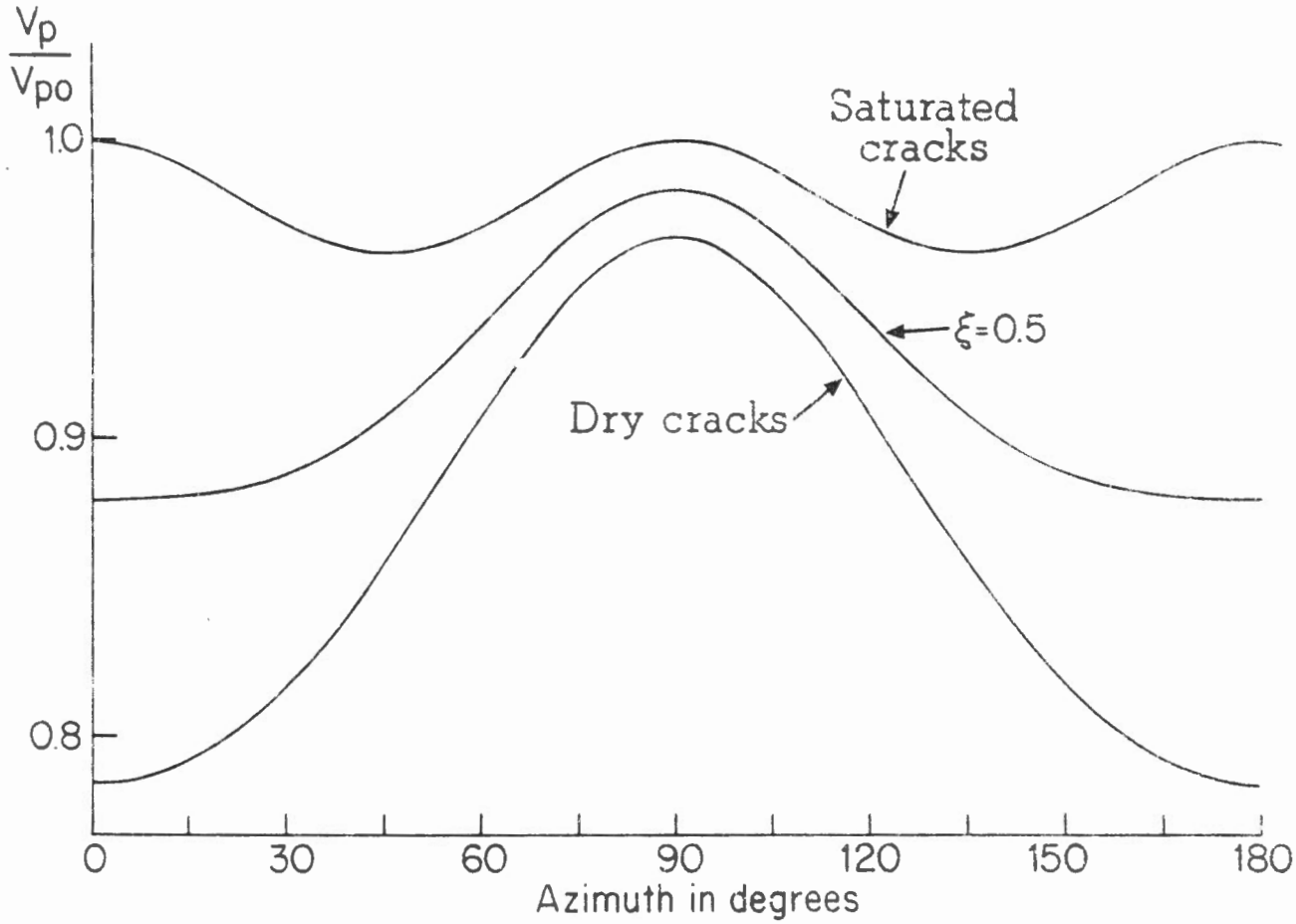

Fig. 6 Seismic anisotropy produced by aligned cracks after Crampin et al. (1980). V_{po} is the seismic velocity of the rock matrix.

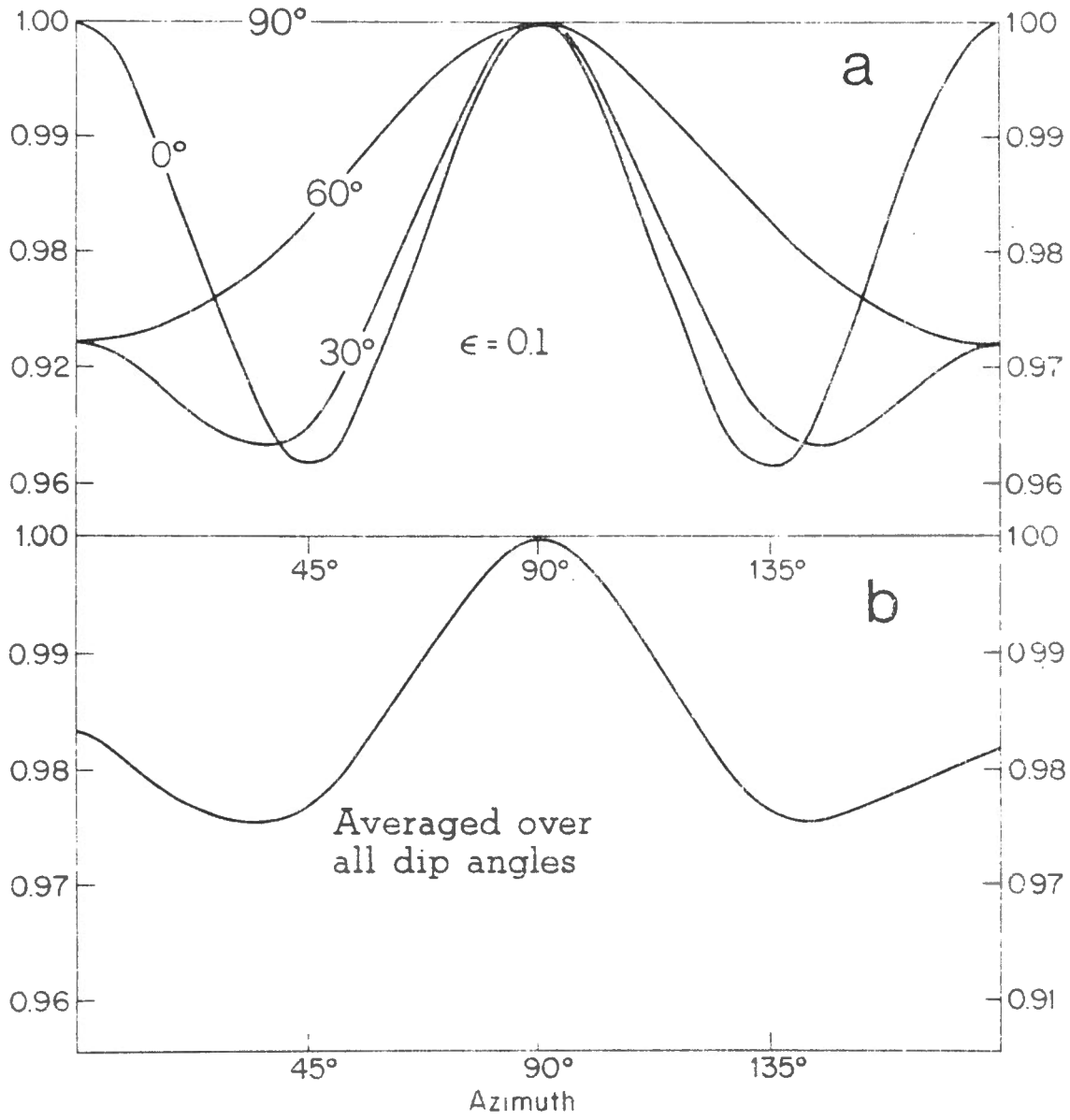

Fig. 7 Seismic anisotropy produced by aligned cracks for various dip angles.

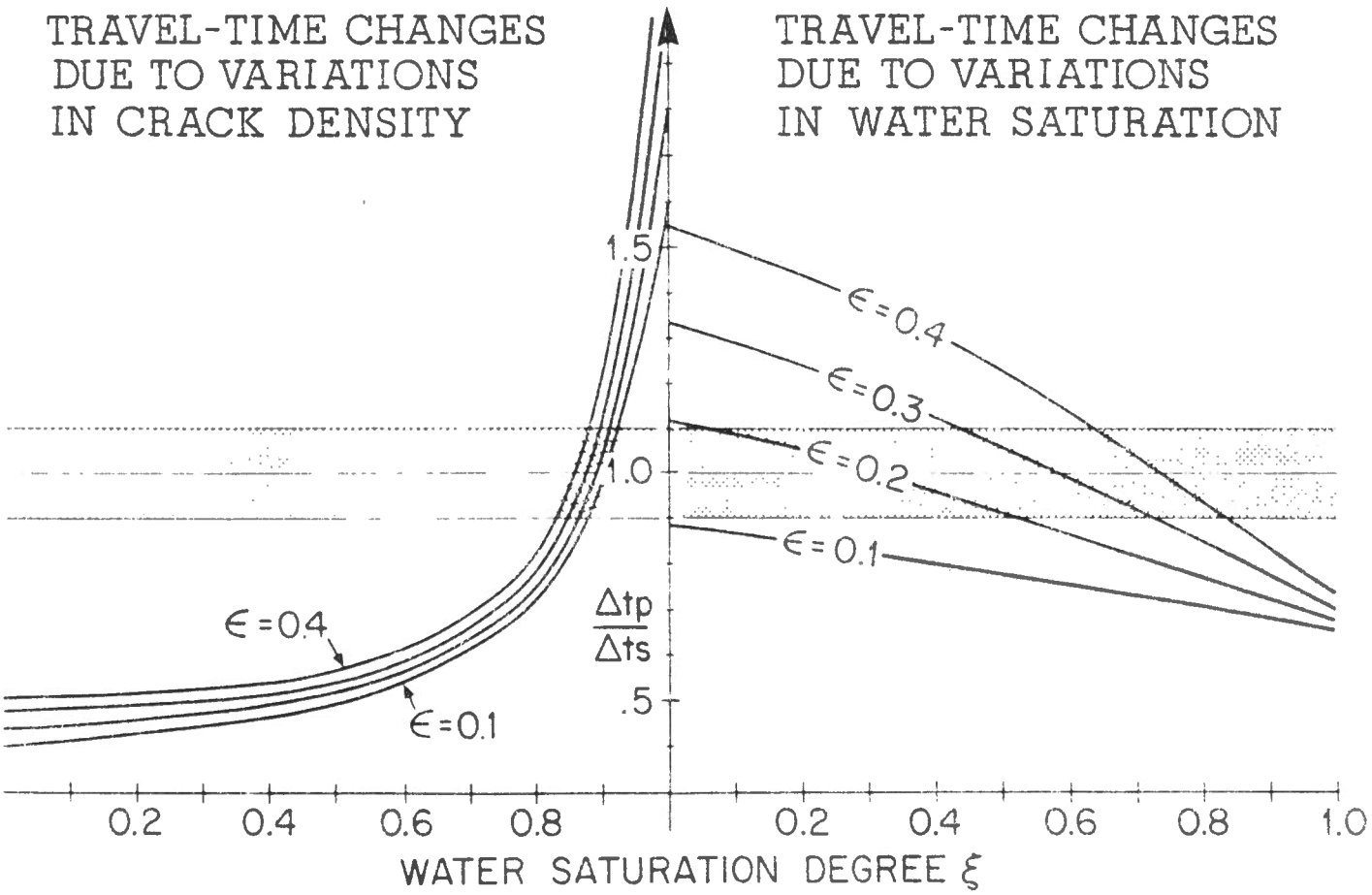

Fig. 8 Changes of traveltime residuals due to changes in crack density and water saturation. Left panel shows $(\Delta t_p/\Delta\varepsilon)/(\Delta t_s/\Delta\varepsilon)$. Right panel shows $(\Delta t_p/\Delta\xi)/(\Delta t_s/\Delta\xi)$.

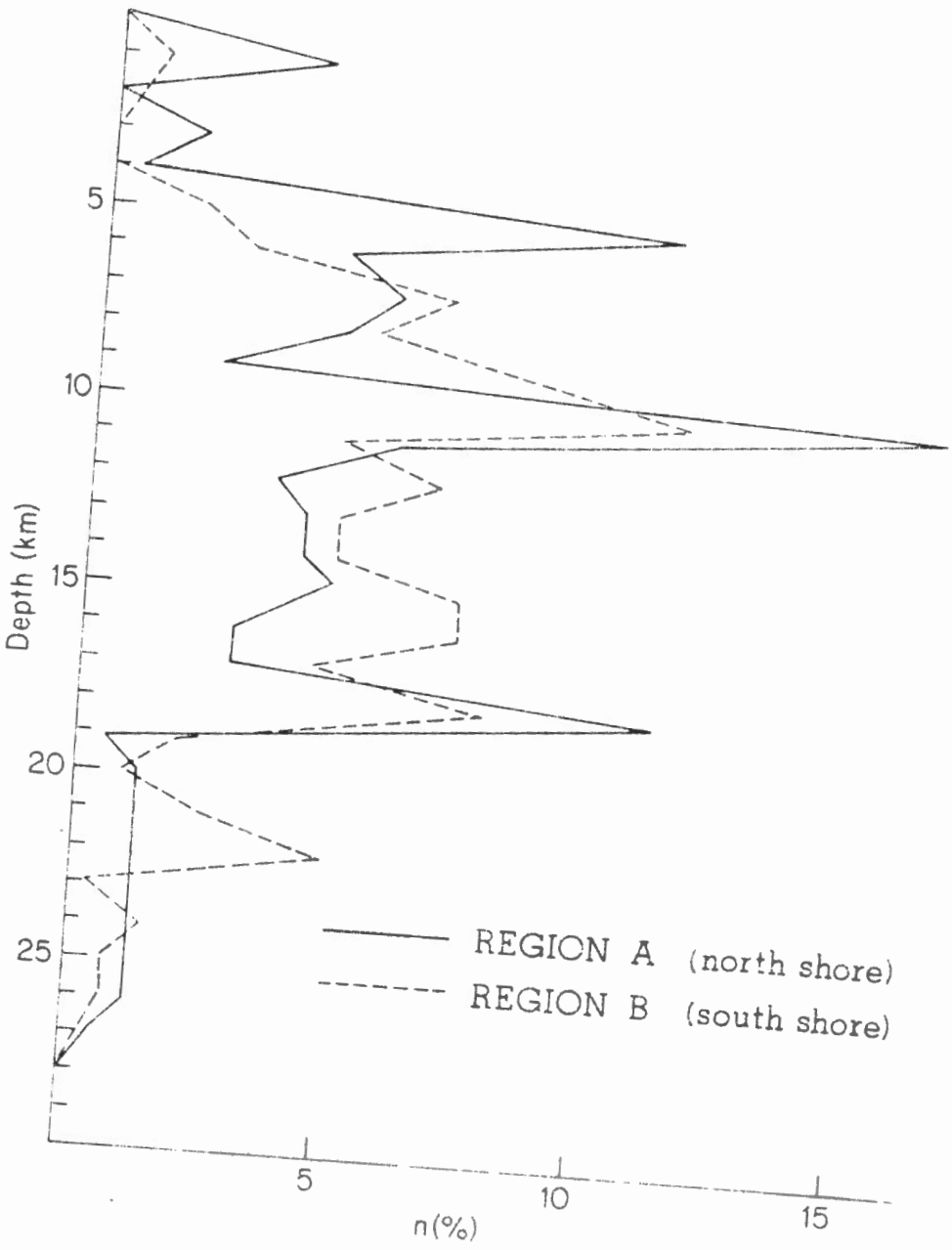

Fig. 9 Depth-frequency distribution of earthquakes in the Charlevoix region 1978 - 1982, magnitude up to 5.0 .

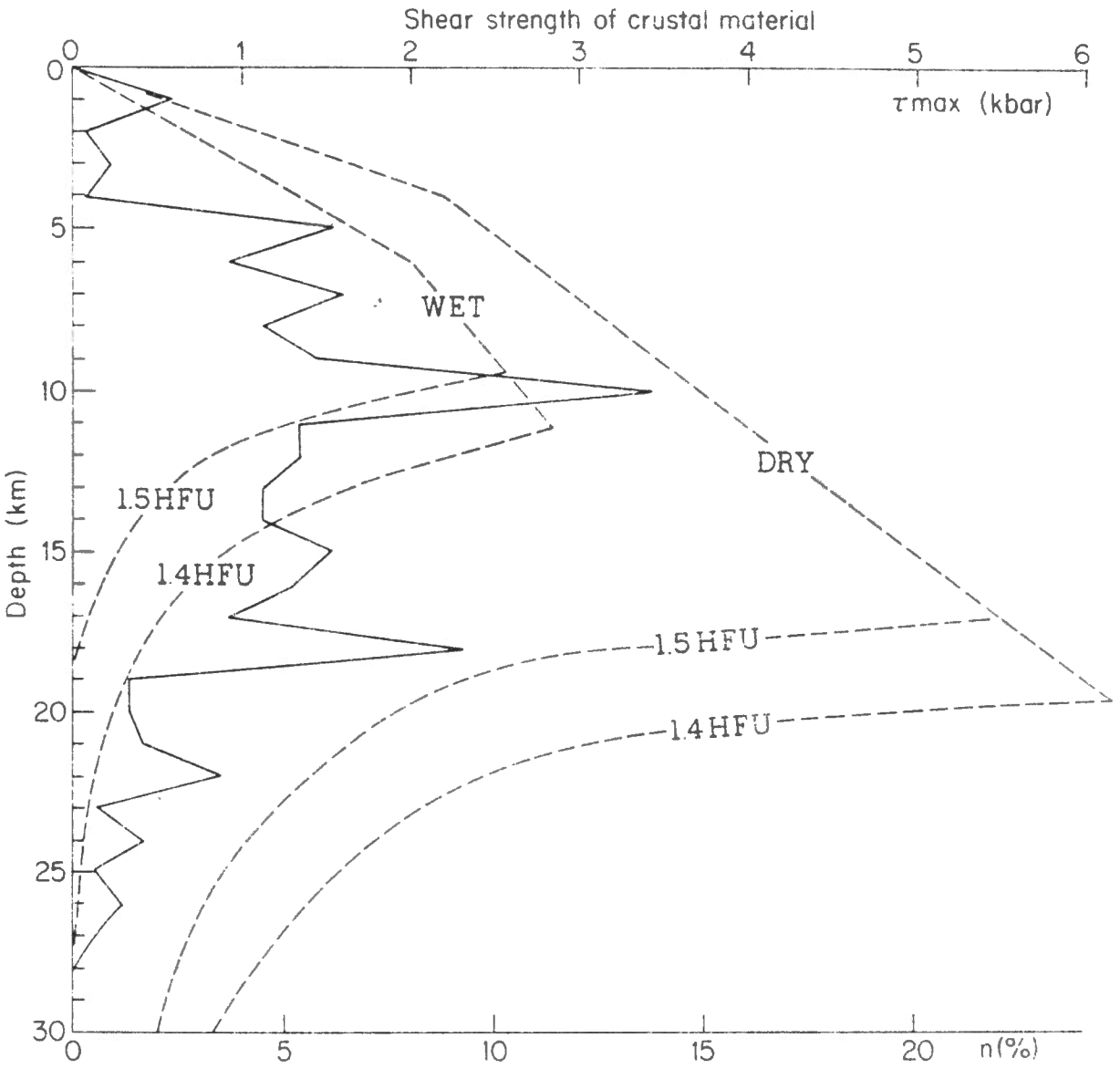

Fig. 10 Depth-frequency distribution of earthquakes in the Charlevoix region and the strength vs depth curves for dry and wet crustal material after Meissner and Strehlau (1982).

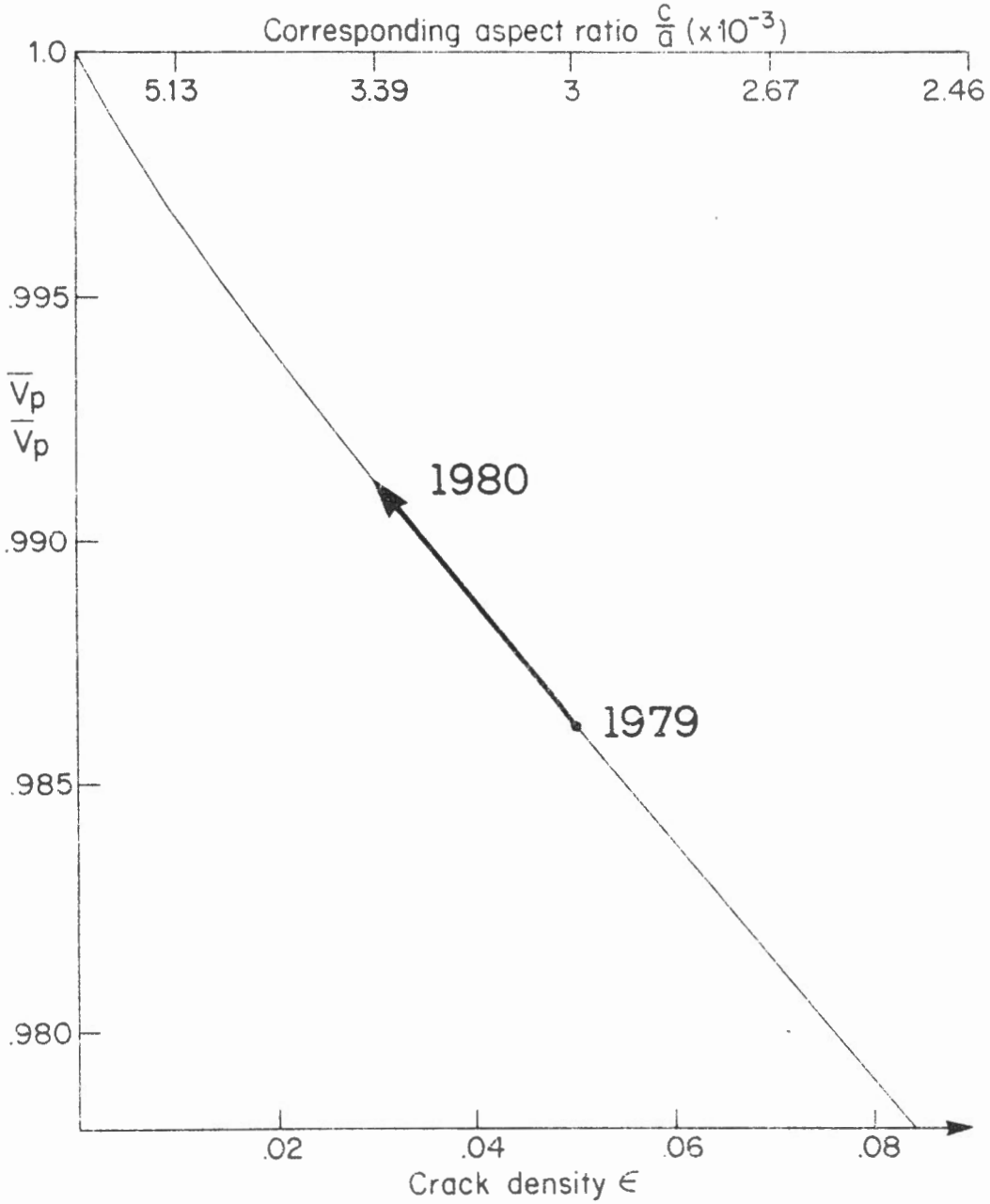

Fig. 11 Seismic velocities for cracked rock under the assumption of cracks opening with constant width (after O'Connell and Budiansky, 1974).

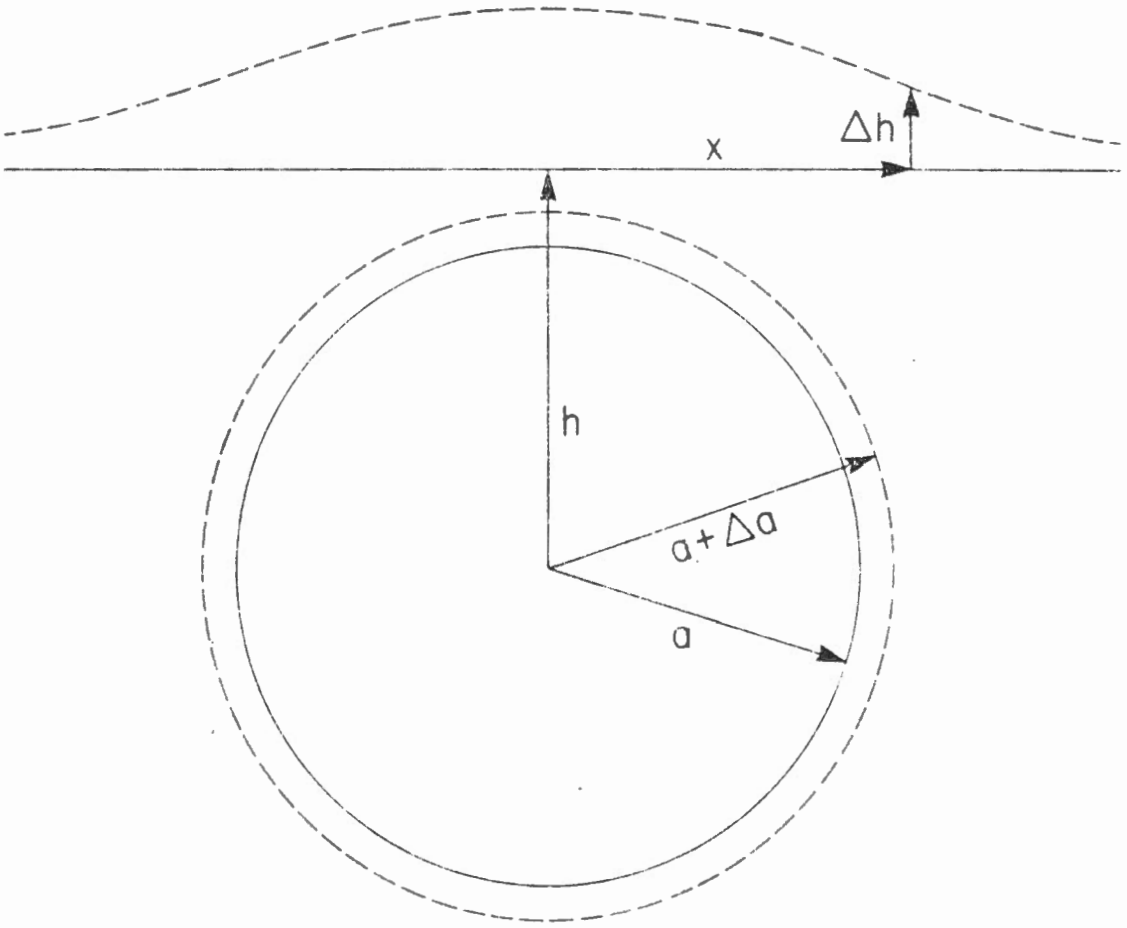

$$\Delta h = \frac{2(\lambda+2\mu)}{\lambda+\mu}\, a^2 \Delta a \frac{h}{\sqrt{(x^2+h^2)^3}}$$

HAGIWARA, 1977

Fig. 12 Notation for the calculation of uplift due to an expanding sphere after Hagiwara (1977).

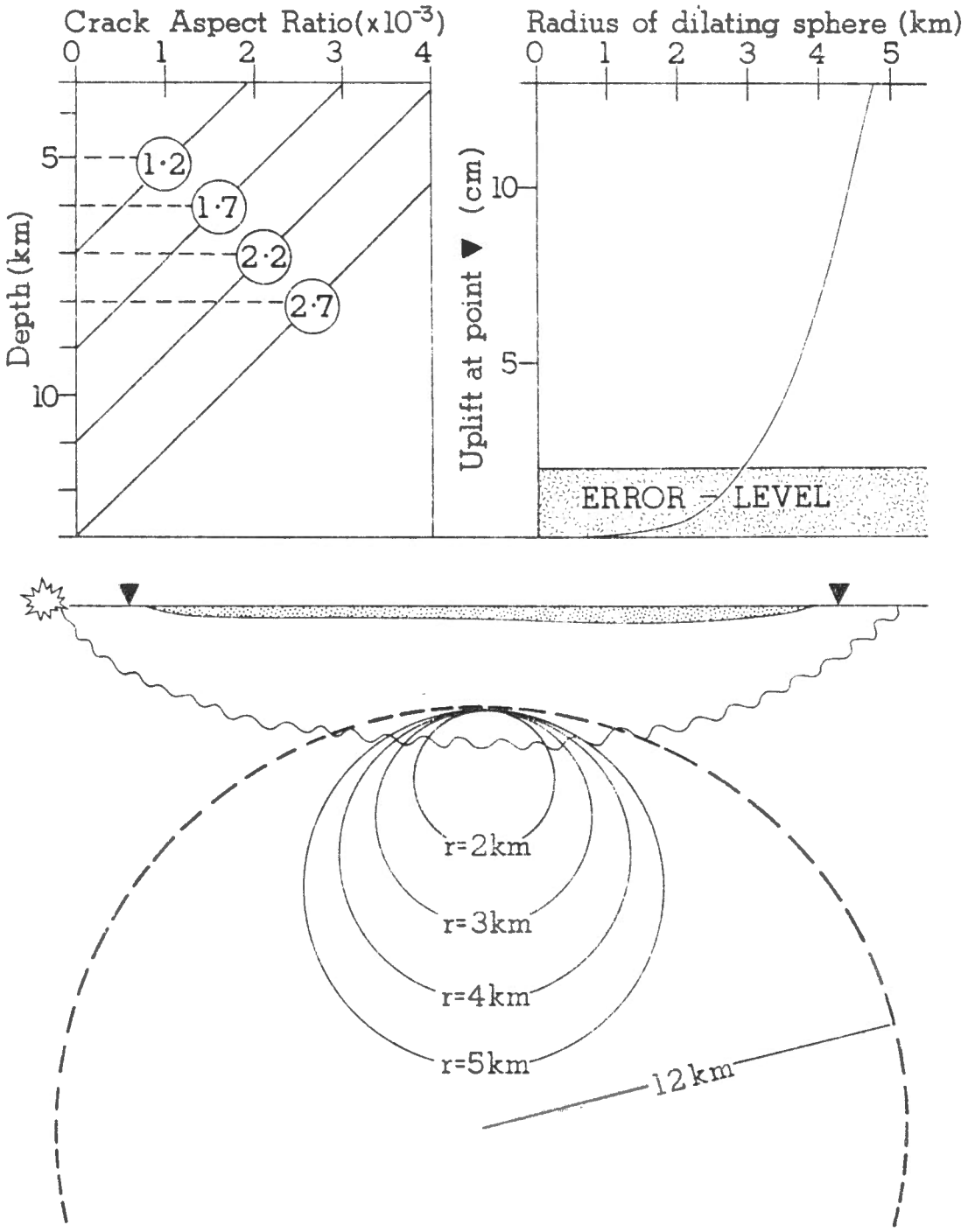

Fig. 13 Calculation diagram for the uplift produced by a crack bearing sphere.

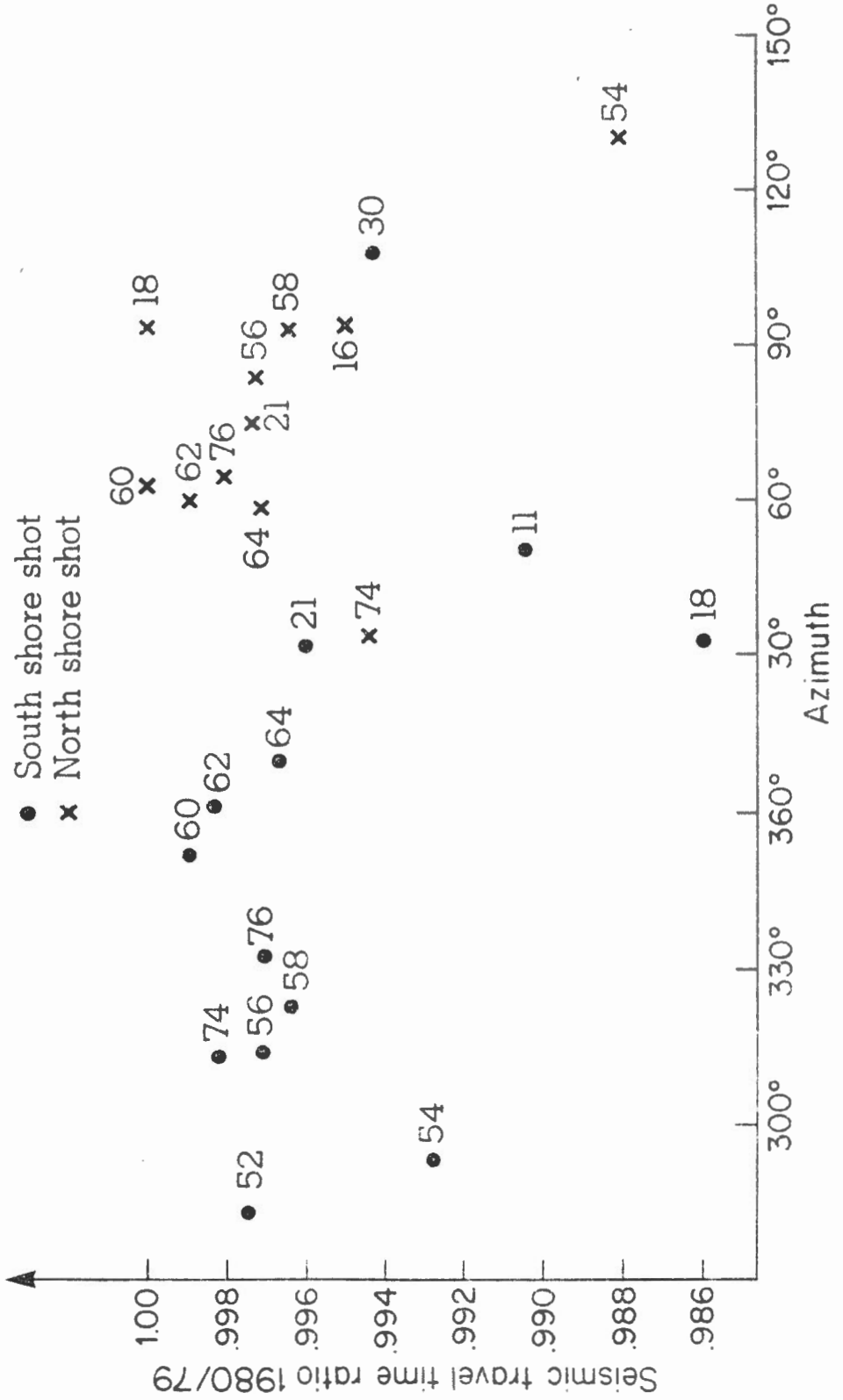

Fig. 14 Traveltime ratio (1979-1980) vs raypath azimuth for all seismometer sites.

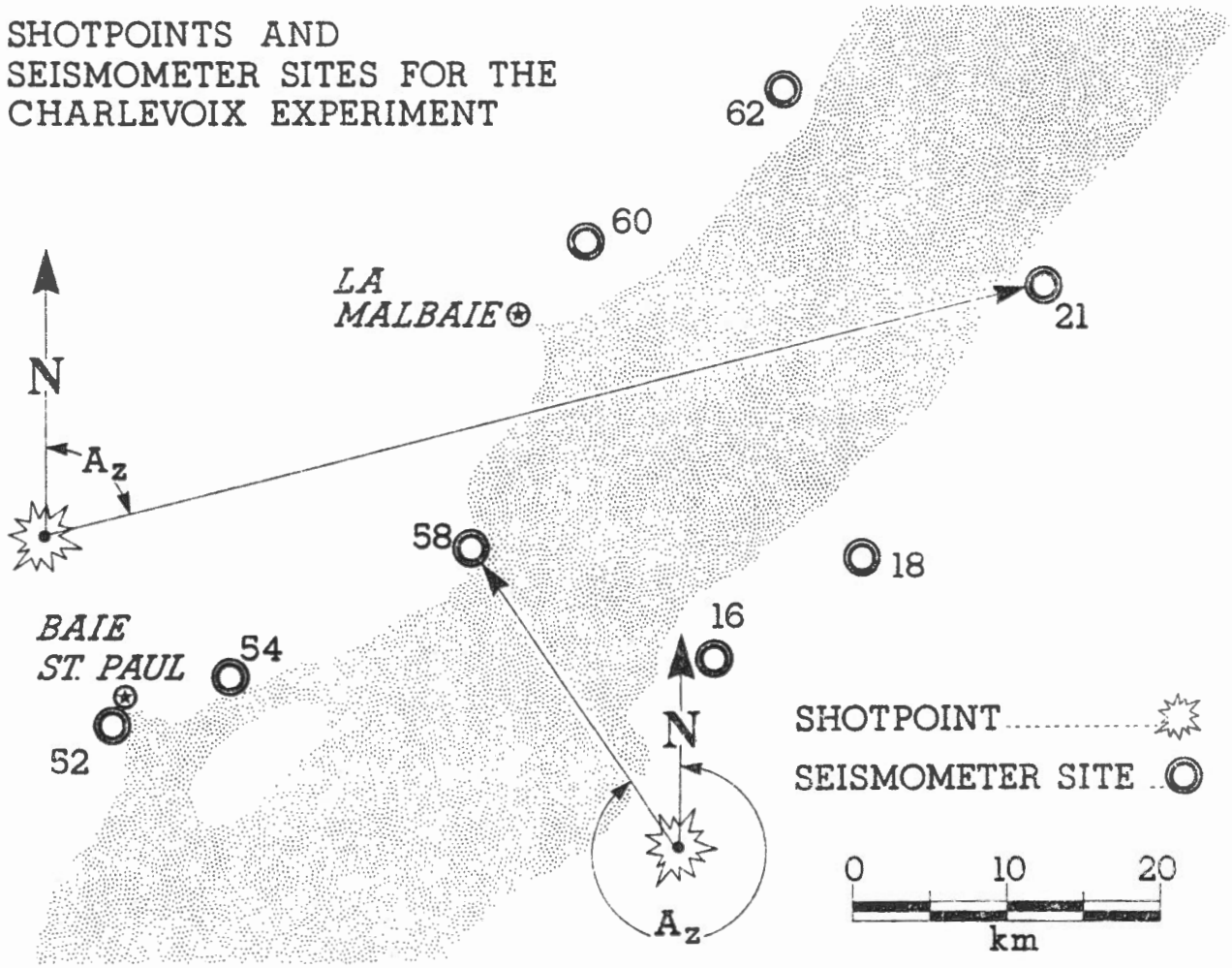

Fig. 15 Definition of raypath azimuth.

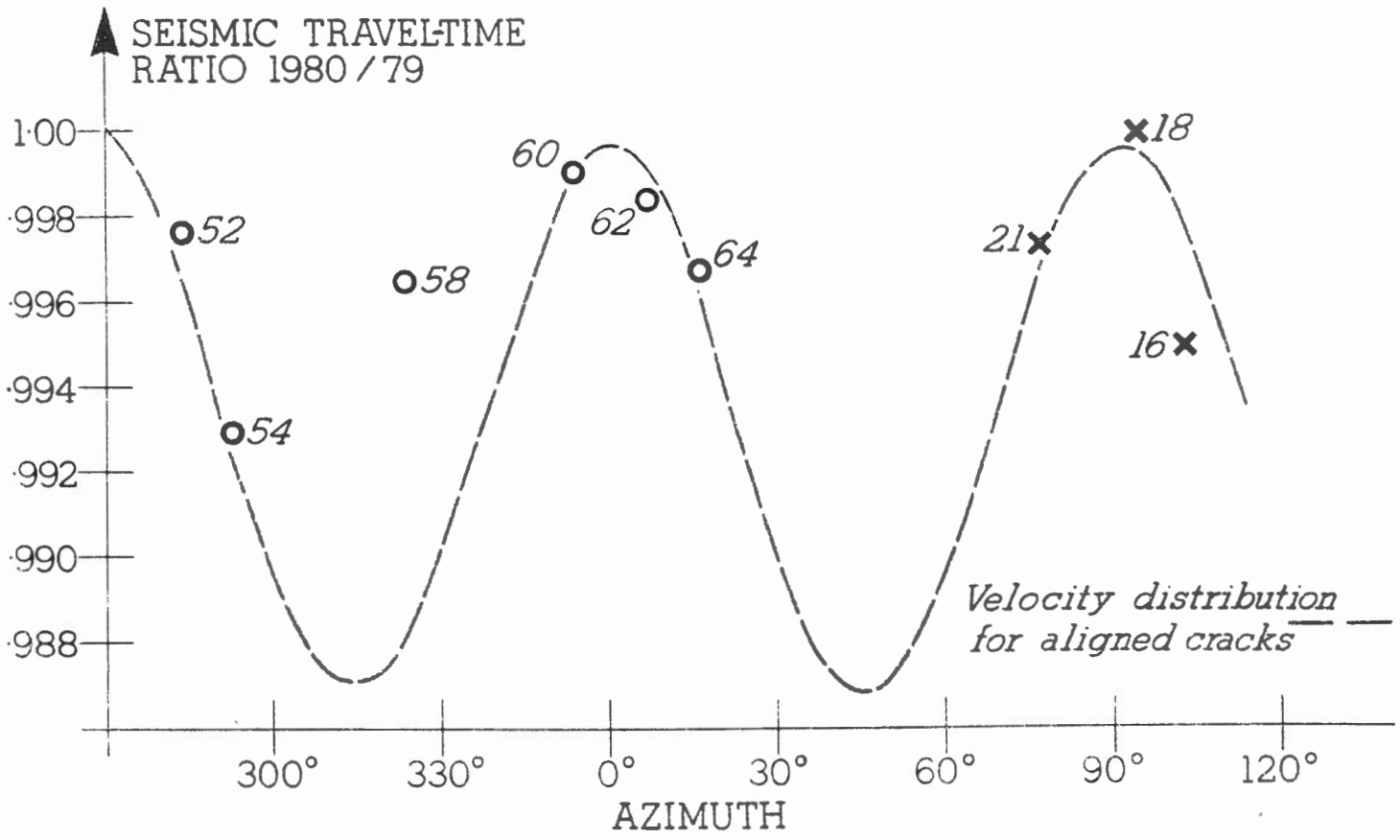

Fig. 16 Traveltime ratio (1979-1980) vs raypath azimuth for raypaths crossing the St. Lawrence River fitted by theoretical values for aligned vertical saturated cracks. Open circles are for raypaths from southshore shots; crosses are for raypaths from northshore shots.

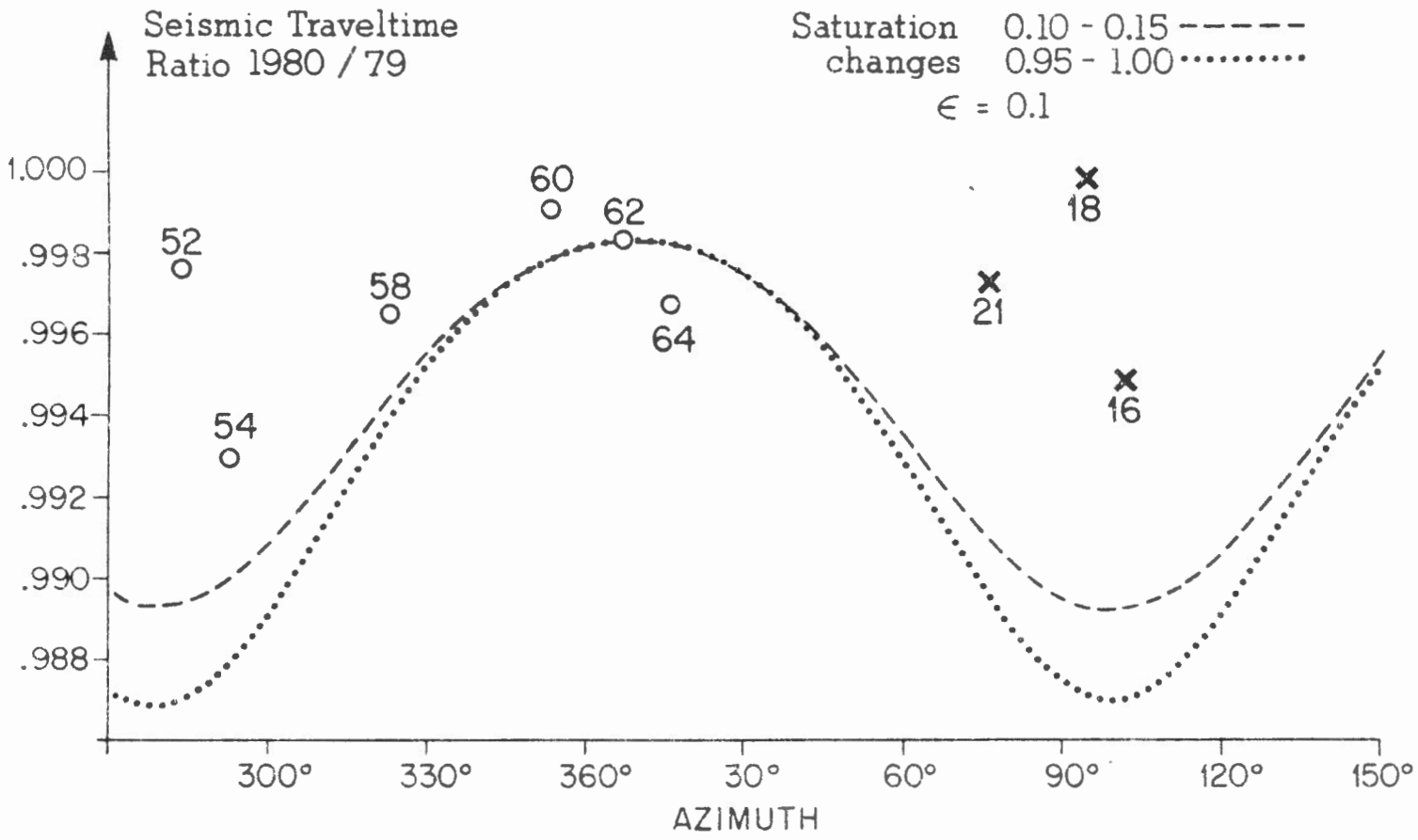

Fig. 17 Attempt to fit the data of Fig. 16 by theoretical values for aligned not totally saturated or nearly dry cracks.

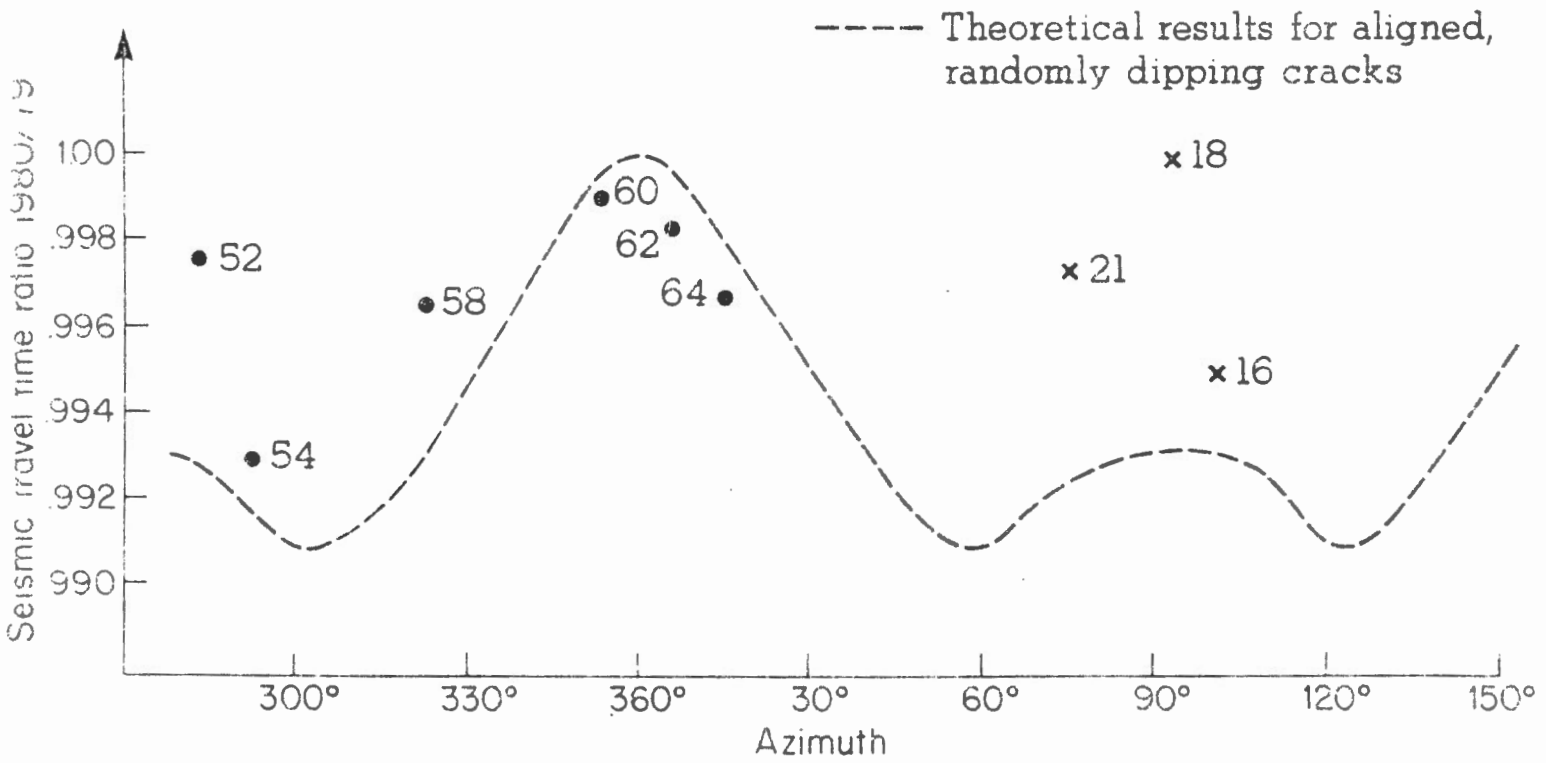

Fig. 18 Attempt to fit the data of Fig. 16 by theoretical values for aligned, but randomly dipping cracks.

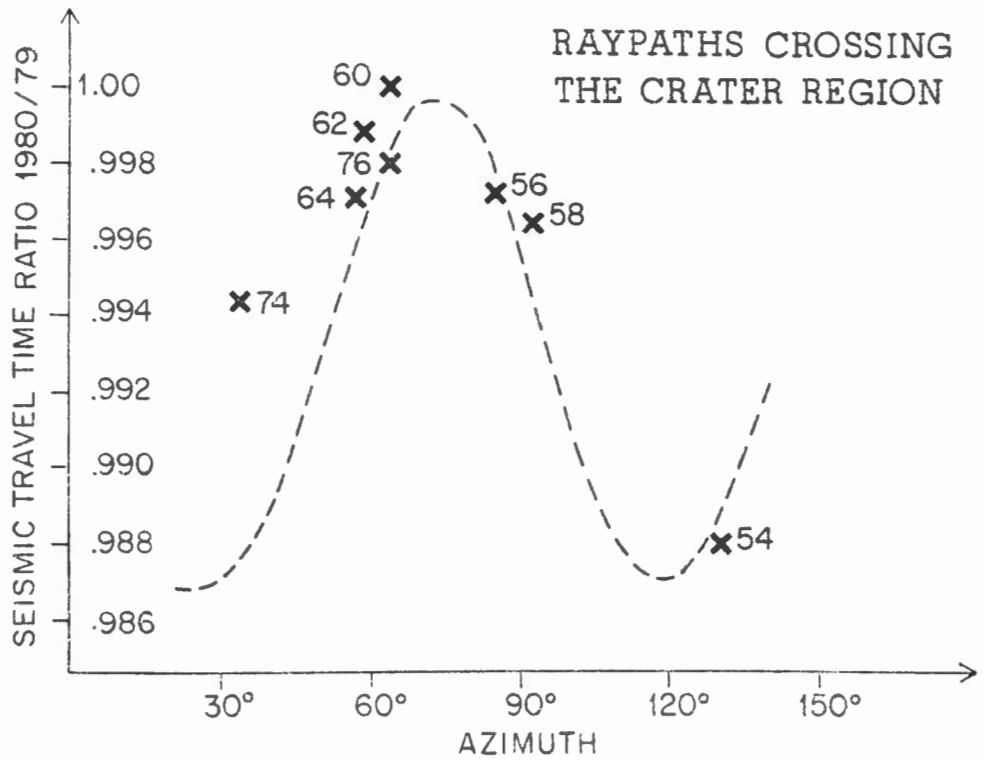

Fig. 19 Traveltime ratio (1979-1980) vs raypath azimuth for raypaths crossing the crater region fitted by theoretical values for aligned vertical saturated cracks.

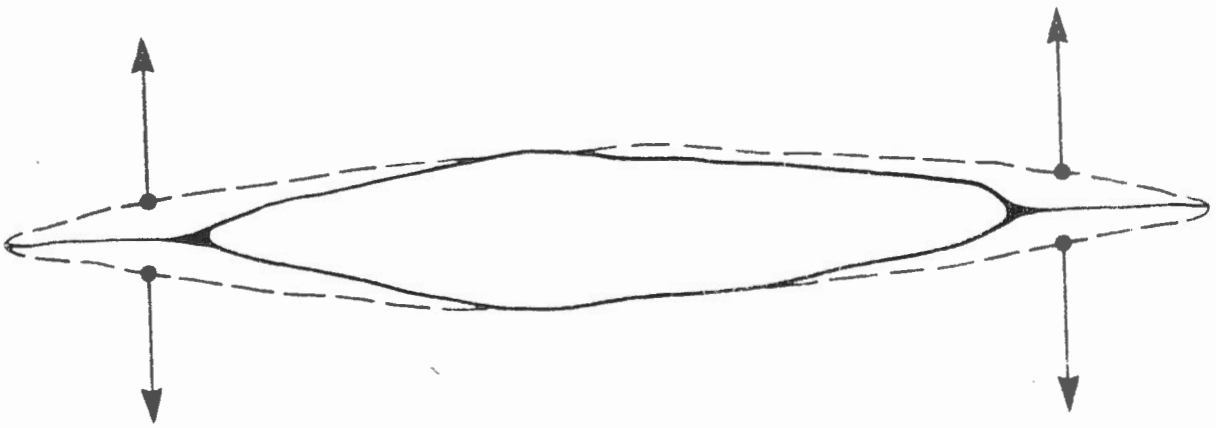

Fig. 20 A crack opening under the influence of external stress and its representation by a double force without moment.

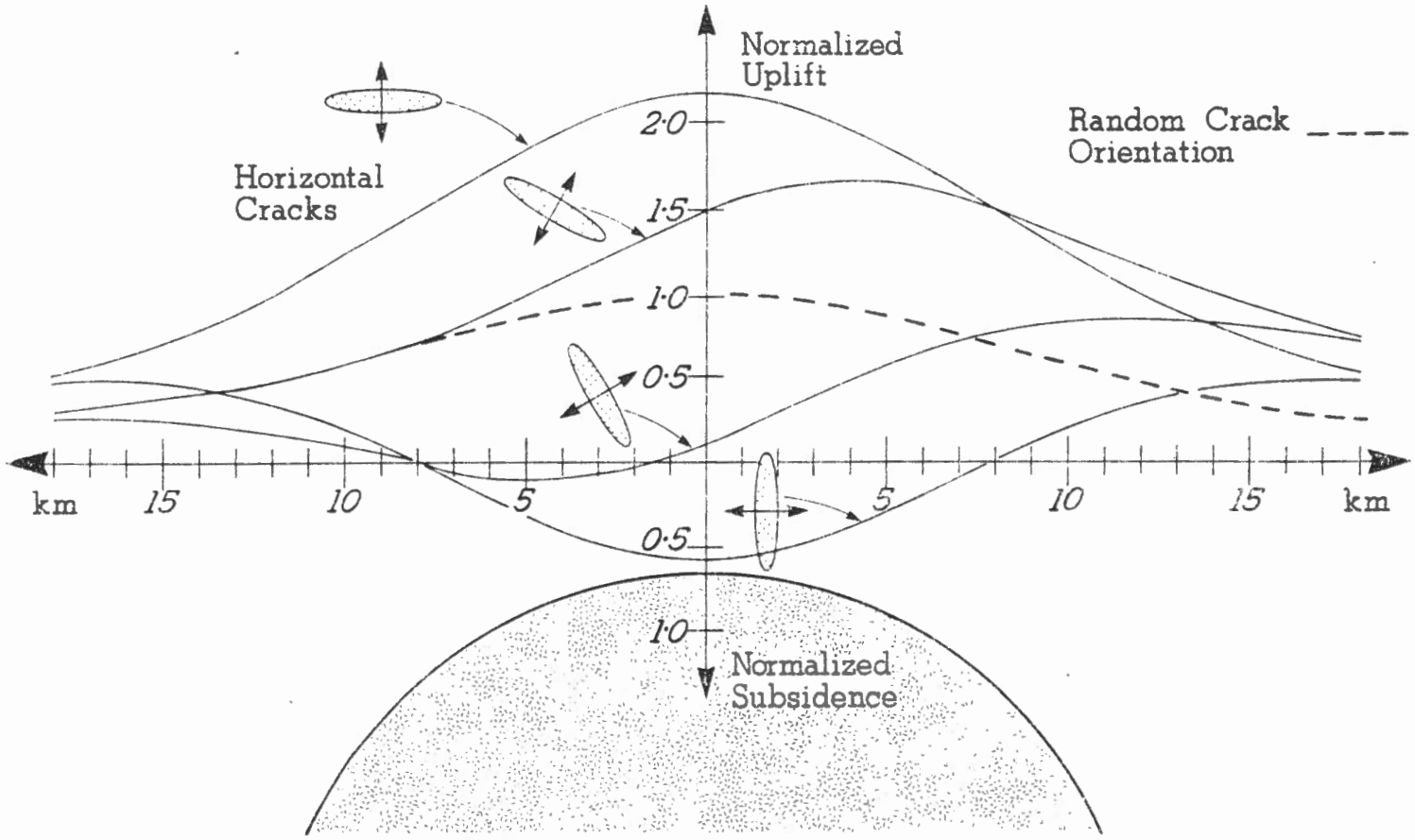

Fig. 21 Normalized vertical motion produced by opening aligned cracks with different dip angles. The vertical motion profile is in a direction normal to the direction of crack extension or contraction.

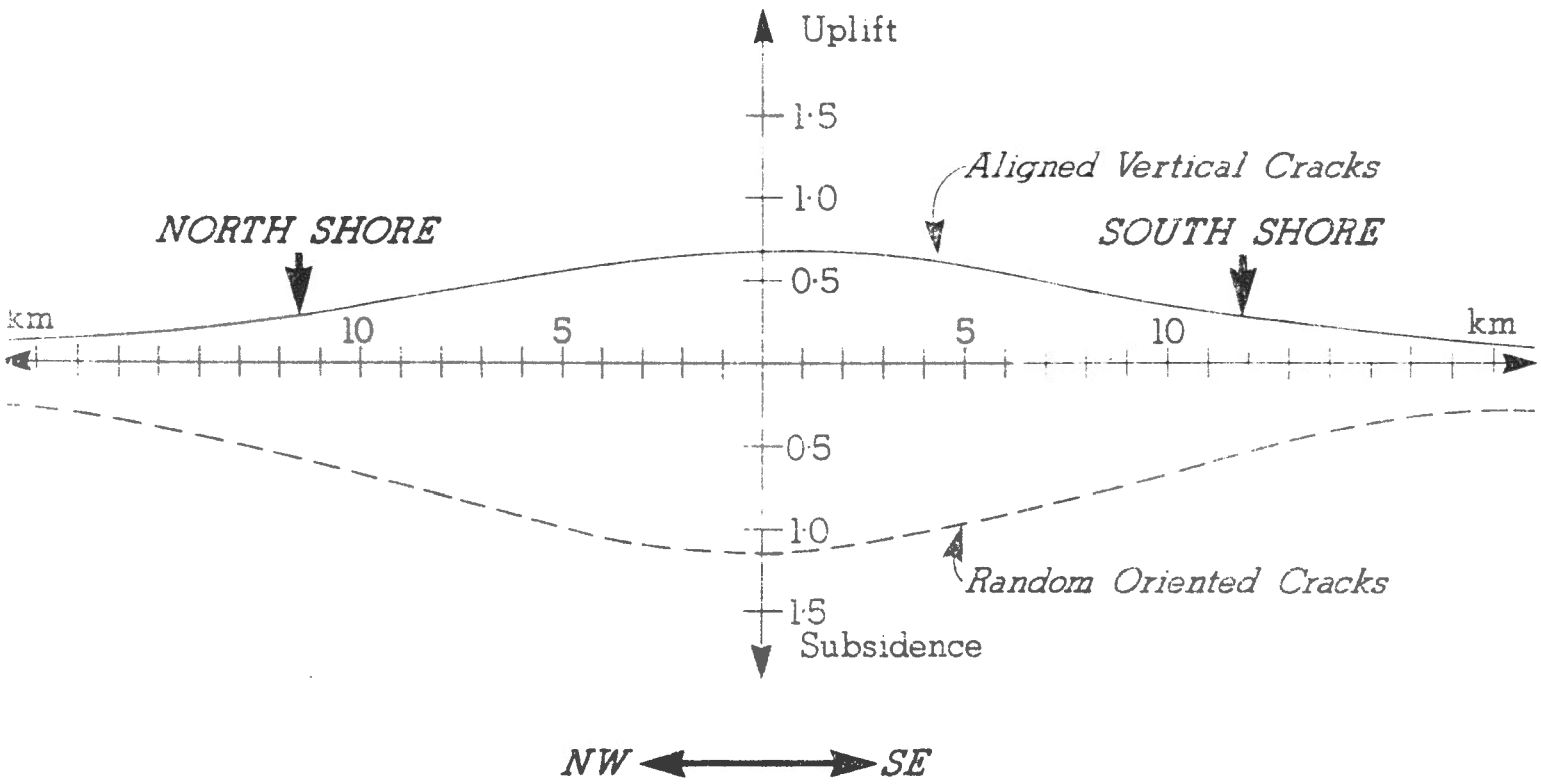

Fig. 22 Comparison of vertical motion produced by aligned and randomly oriented cracks. The profile is parallel to the direction of crack extension or contraction.

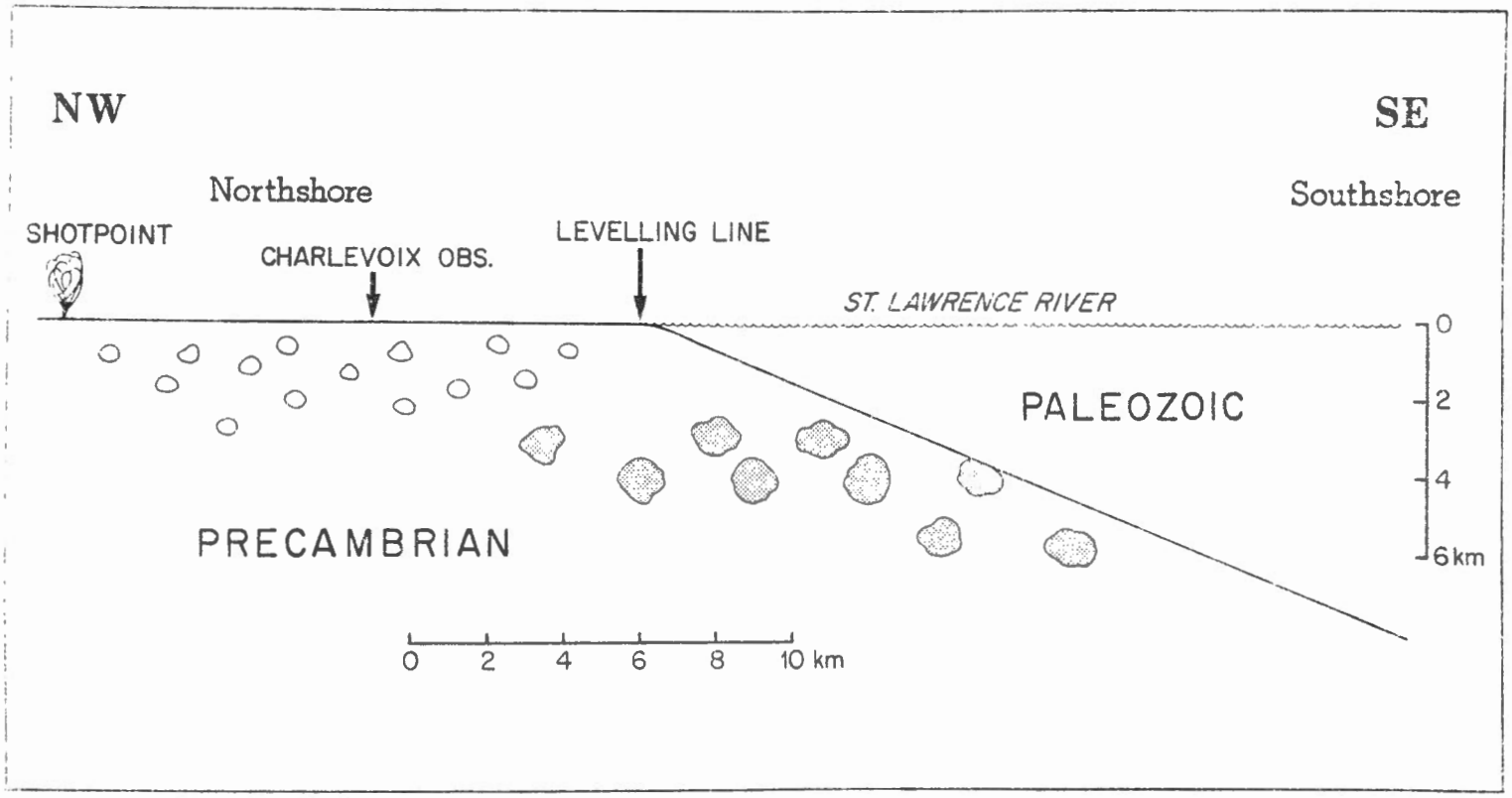

Fig. 23 The multiple inclusion model for the Charlevoix region seen from a SE direction.

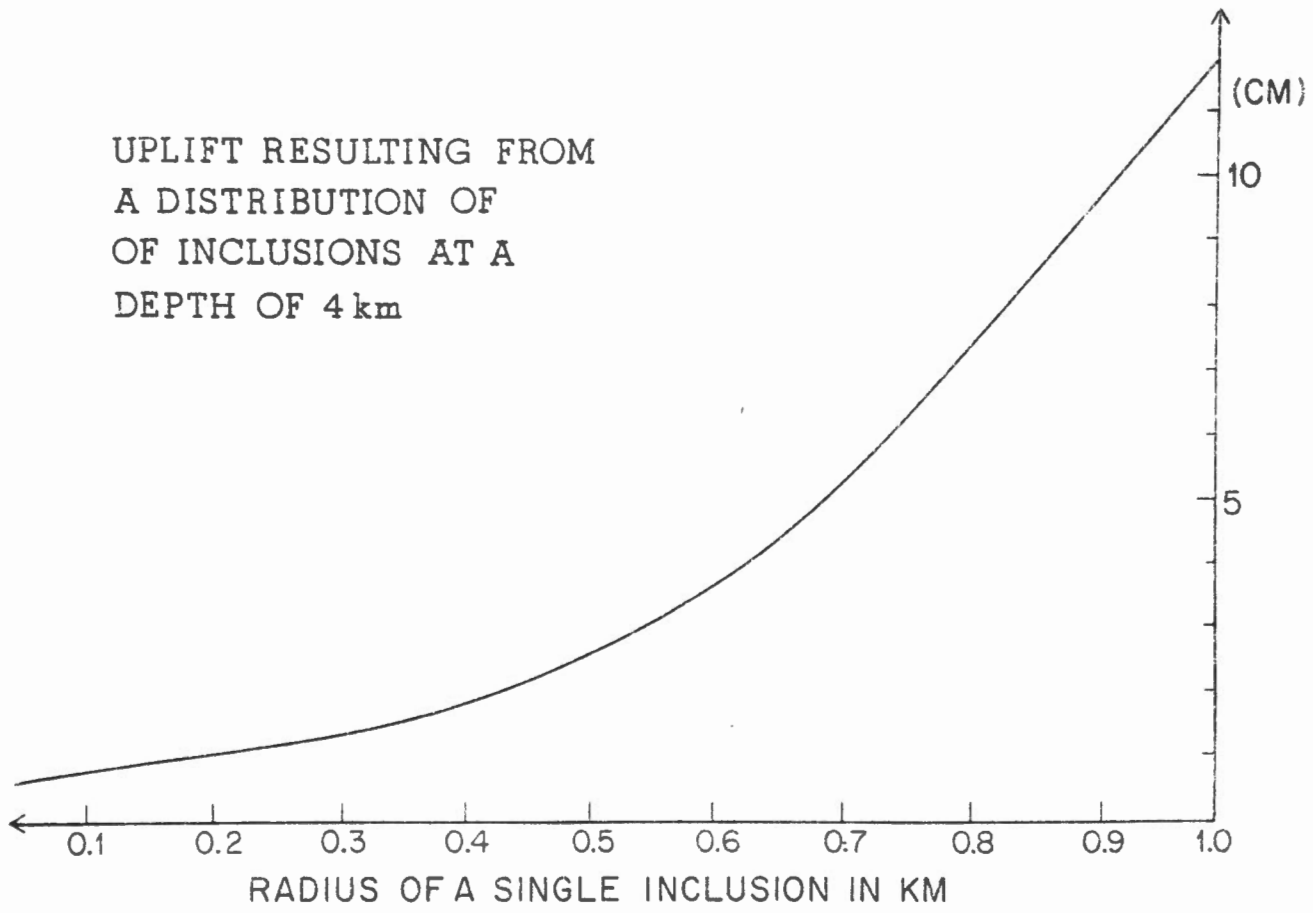

Fig. 24 Vertical motion caused by a regular distribution of crack bearing inclusions spaced 3 km apart.

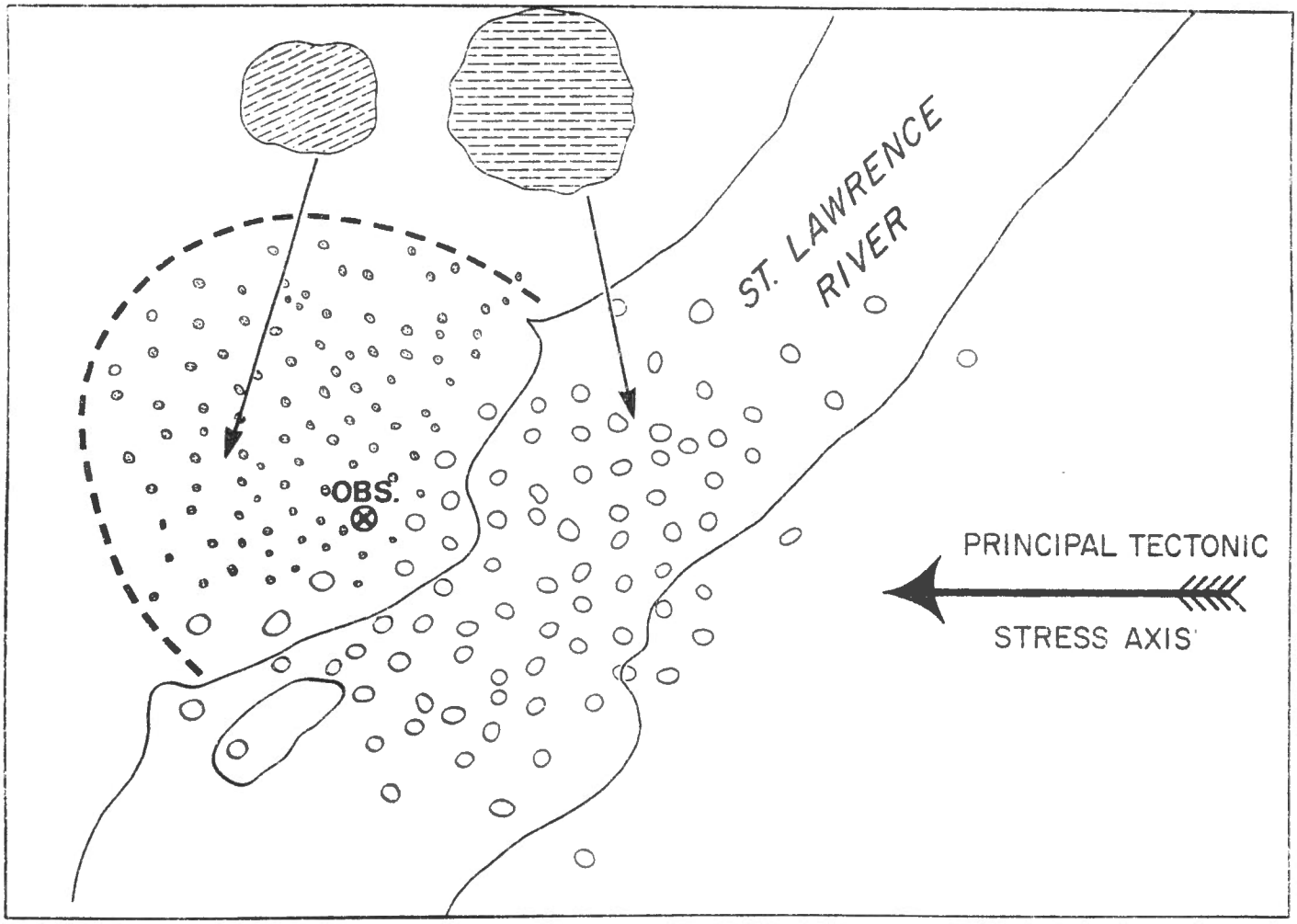

Fig. 25 Plan view of the proposed distribution of inclusions, crack orientation and tectonic stress axis in the Charlevoix region.